Morphodynamics of boulder-bed semi-alluvial streams in northern Fennoscandia: a flume experiment to determine sediment self-organization

L. E. Polvi[1]

[1]Department of Ecology & Environmental Science, Umeå University, Umeå, 907 36 Sweden

Corresponding author: Lina E. Polvi (lina.polvi@umu.se)

Key Points:

- Boulder-bed semi-alluvial channels behave like low submergence regime mountain streams with sediment deposition upstream of boulders

- Fennoscandian semi-alluvial rapids are not re-worked (boulders transported or bedform formation) by high fluvial flows (i.e., Q_{50})

- Large grains ($>D_{84}$) are important in shaping channel morphodynamics and have implications for restoration of salmonid spawning gravel

Abstract

In northern Fennoscandia, semi-alluvial boulder-bed channels with coarse glacial legacy sediment are abundant and due to widespread anthropogenic manipulation during timber-floating, unimpacted reference reaches are rare. The landscape context of these semi-alluvial rapids— with numerous mainstem lakes that buffer high flows and sediment connectivity in addition to low sediment yield— contribute to low amounts of fine sediment and incompetent flows to transport boulders. To determine the morphodynamics of semi-alluvial rapids and potential self-organization of sediment with multiple high flows, a flume experiment was designed and carried out to mimic conditions in semi-alluvial rapids in northern Fennoscandia. Two slope setups (2% and 5%) were used to model a range of flows (Q_1, Q_2, Q_{10} & Q_{50}) in a 8 x 1.1 m flume with a sediment distribution analogous to field conditions; bed topography was measured using structure-from-motion photogrammetry after each flow to obtain DEMs. No classic steep gravel-bed channel bedforms (e.g., step-pools) developed. However, similarly to boulder-bed channels with low relative submergence, at Q_{10} and Q_{50} flows, sediment deposited upstream of boulders and scoured downstream. Because the Q_{50} flow could not re-work the channel by transporting boulders or forming channel-spanning boulders, the channel-forming discharge is likely larger than the Q_{50}. These results have implications for restoration of gravel spawning beds in northern Fennoscandia and highlight the importance of large grains in understanding channel morphodynamics.

Plain language summary

Many streams in northern Scandinavia and Finland contain abundant boulders that were originally deposited by glaciers (>10,000 year ago). However, most of these so-called 'semi-alluvial' streams were heavily altered during the timber-floating era. In order to understand how these streams should look naturally and change over time, experiments were conducted mimicking this stream type. An experimental stream was built in a flume (8 x 1.1 m) with down-scaled sediment sizes matching that of real streams in northern Sweden. With two different slopes (2% and 5%), four flows were run to mimic flows ranging from the annual high flow to the 50-year flood. Because lakes are common along these streams, high recurrence-interval flows (that occur rarely) are not as large as in mountain streams. Therefore, boulders barely moved even with the 50-year flood at the 2% slope and only rolled slightly at the 5% slope (due to downstream scour). During 10-year and 50-year floods, finer sediment deposited upstream and eroded downstream of boulders. Contrary to mountain streams with coarse boulders, a flow much greater than the 50-year flood is necessary to re-work the channel bed. These results have implications for stream restoration, providing habitat and spawning gravel for trout and salmon.

1 Introduction

1.1 Semi-alluvial channels

Semi-alluvial channels have commonly been described as those where a cohesive boundary, most commonly bedrock or cohesive clays, either composes the channel banks, thus

56 confining the channel from lateral migration, or the channel bed, thus constraining the channel
57 from degrading (Coulombe-Pontbriand & LaPointe, 2004; Meshkova et al., 2012; Turowski,
58 2012). Another type of semi-alluvial channel exists where the channel contains abundant
59 cohesive or coarse sediment, which are fixed immobile points in the channel and have not been
60 deposited by alluvial processes (Pike et al., 2018). This potentially immobile sediment has been
61 referred to either as lag or legacy deposits in cases where mass wasting has caused an input of
62 coarser material (e.g., Brummer & Montgomery, 2003), where lahar deposits below the channel
63 inhibits incision (Reid et al., 2013), where a previous geomorphic process regime, such as
64 glaciation, has deposited sediment that is currently immobile within the current fluvial
65 hydrological regime (Gran et al., 2013; Polvi et al., 2014). Semi-alluvial channels with glacially-
66 derived sediment from depositional landscapes formed by continental ice sheets may contain
67 non-alluvial patches that are (1) easily eroded and form alluvial deposits, (2) cohesive fine-
68 grained material that only responds to extreme high flows (Pike et al. 2018), or (3) coarse-
69 grained cobbles and boulders (Ashmore & Church, 2001; Polvi et al., 2014). Such semi-alluvial
70 channels with till beds, containing either cohesive sediment or sand, gravel and large boulder
71 clasts, are common on Canada's Southern Shield and Southern Boreal Shield (Ashmore &
72 Church, 2001) and in northern Fennoscandia (Polvi et al., 2014). In such systems, where all
73 sediment was not deposited by fluvial processes and is potentially unable to be reworked even by
74 low recurrence-interval high flows, it is unknown whether the mobile sediment self-organizes
75 into predictable bedforms or whether predictable patterns of sediment clusters and scour are
76 form.

77 In northern Fennoscandia, boulder-bed semi-alluvial channels are common (Polvi et al.
78 2014; Rosenfeld et al., 2011), as the landscape has been shaped by several episodes of
79 continental glaciation. Glacially drifted till is the most common deposit in Fennoscandia,
80 forming various landforms in the form of ribbed and Rogen moraines, drumlins, eskers, and
81 erratics (Seppälä, 2005). Semi-alluvial channels are found in tributary catchments to large rivers
82 that flow from the mountains to the Baltic Sea in areas with mapped fluvio-glacial sediment in
83 longitudinal swaths (Geological Survey of Sweden surficial geology maps, 1:25,000- 1:100,000).
84 The tributaries are divided into three main process domains, which are spatially separate zones
85 with distinct suites of geomorphic process (*sensu* Montgomery, 1999): lakes, slow-flowing
86 reaches in peat or fine sediment (S_0: <0.01 m/m), and semi-alluvial rapids (S_0: 0.005-0.07 m/m)
87 (Figure 1). Similar systems with abundant mainstem lakes and 'steeps' and 'flats' have been
88 described by Snyder et al. (2008, 2012) in a similarly glaciated landscape in Maine, USA.
89 Putting semi-alluvial rapids within the context of their stream network organization of process
90 domains is necessary to understand reach-scale sediment processes. Mainstem lakes buffer
91 sediment and water fluxes, which reduce the available fine sediment input from upstream reaches
92 (Snyder et al., 2012) and may preclude very high flows (Leach & Laudon, 2019). Thus, to
93 summarize, a process-based understanding of morphodynamics in semi-alluvial rapids in
94 northern Fennoscandia is hampered by two geomorphic factors: (1) streams are semi-alluvial, in
95 that they contain coarse glacial lag sediment (till from moraines and subglacial tunnels) and (2)
96 numerous mainstem lakes buffer sediment and water fluxes.

97 Furthermore, natural reference sites are lacking due to extensive timber-floating (mid
98 1800s to ~1980) that caused widespread channelization and clearing of rapids, so stream
99 restoration schemes cannot rely on copying existing reference sites. In these rapids, some of
100 which were unimpacted and others of which were channelized and later restored, no clear pool-

101 riffle or step-pool bedforms have been observed in the field (*personal observation*), and cascade
102 bedforms have been observed at slopes where plane bed, alternate bar, or step-pools should form
103 in alluvial channels (S_0: ~0.04-0.07 m/m, *sensu* Montgomery & Buffington, 1997; Palucis &
104 Lamb, 2017). Due to the widespread nature of timber-floating, which necessitated channelization
105 and clearing of coarse boulders (through manual clearing, the use of dynamite and bulldozers),
106 virtually no unimpacted reference reaches exist (Nilsson et al., 2005). Most of those that were
107 unimpacted by channelization—though were still impacted by clearing of instream wood,
108 harvesting of old-growth riparian trees, and flow diversion—are steeper than those that have
109 been restored (Polvi et al., 2014). In the past decade, several stream restoration projects have
110 attempted to restore these semi-alluvial rapids because of the low salmonid populations and
111 negative effects on biodiversity (Gardeström et al., 2013); however, very little research or
112 knowledge on the processes governing sediment transport and organization in these streams are
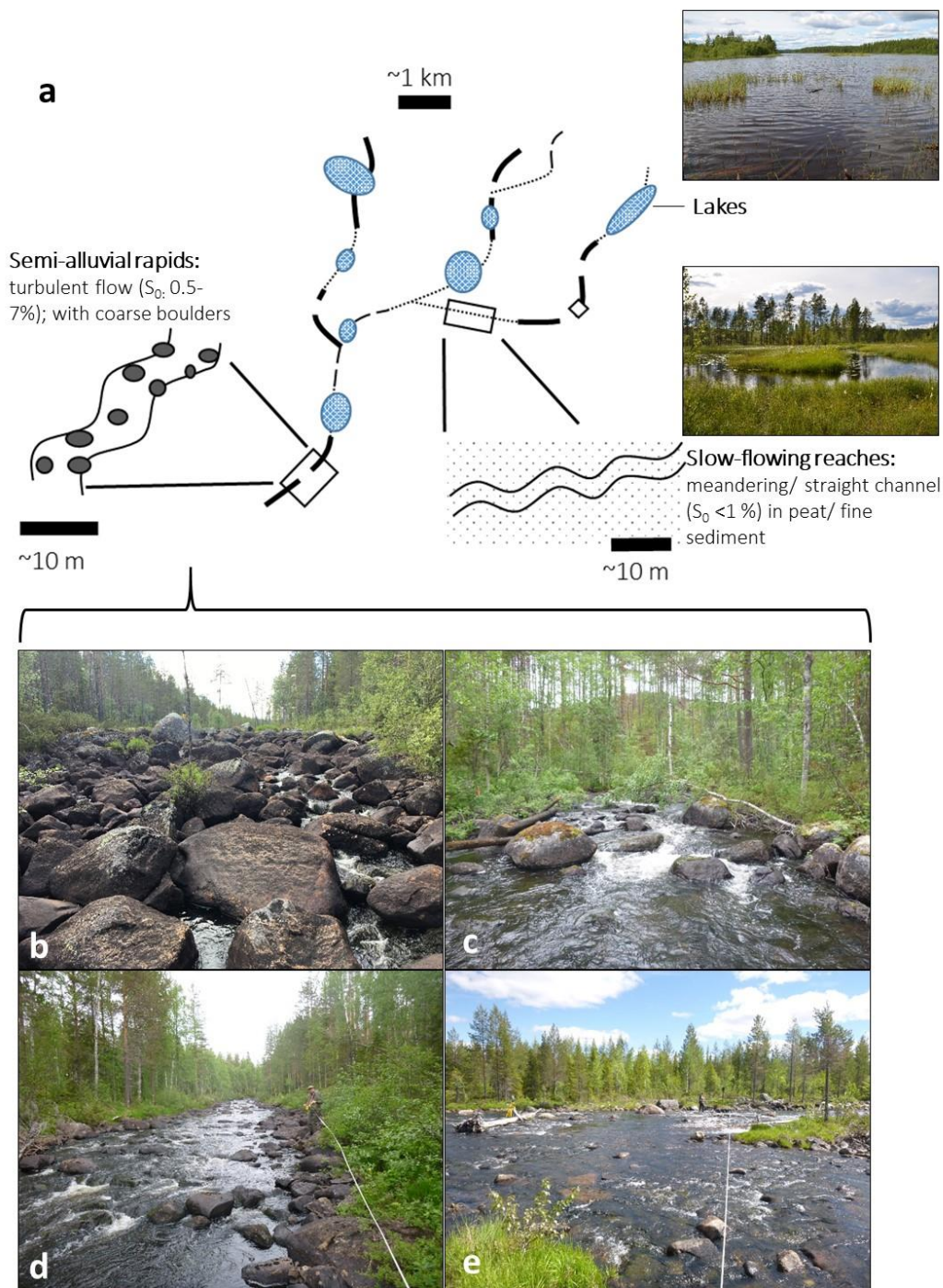113 available (except Rosenfeld et al., 2011).

114

Figure 1. (a) Schematic of stream networks in tributary streams in northern Fennoscandia. Streams are segmented into three process domains: semi-alluvial rapids, slow-flowing reaches and lakes, with four examples of prototype reaches of semi-alluvial rapids (b-e). Photos b & c are of unimpacted reaches with channel bed slopes of 0.05 and 0.04 m/m, respectively; photos d & e are of restored reaches with channel bed slopes of 0.03 and 0.02 m/m, respectively. In photos b-d, the flow direction is out of the picture, and in photo e, the flow direction is from right to left.

122   1.2 Background

123   The channel geometry and bedforms found in semi-alluvial channels are not easily
124 predicted based on slope or bankfull discharge. Forms and processes of alluvial streams, on the
125 other hand, have been well-studied, allowing prediction of sediment transport, channel geometry,
126 and bedforms (Church, 2006; Faustini et al., 2009). For example, regionally-derived downstream
127 hydraulic geometry equations can be used to predict channel width, depth, and velocity based on
128 relationships with bankfull discharge or drainage area, because these channel geometry
129 parameters reflect the stream's equilibrium conditions (Church, 2006; Leopold & Maddock,
130 1953). Even in steep, gravel-bed channels, channel bed slope can accurately predict bedform
131 morphology (e.g., step-pools, plane bed or pool-riffle), which may reflect a balance between
132 sediment supply and transport capacity (Montgomery & Buffington, 1997) or other processes co-
133 varying with slope (Palucis & Lamb 2017). In addition, the formation of and the controlling
134 mechanisms of sediment sorting in step-pools and pool-riffles have been examined, showing that
135 these bedforms reflect a self-organization phenomenon that form in order to dissipate energy
136 (Chin & Wohl, 2005), and that sediment is preferentially stored in and mobilized from pools
137 (e.g, Sear, 1996).

138   Some insight into semi-alluvial channels with coarse glacial sediment are available from
139 experiments based on mountain streams with boulder-bed channels. In general, the effects of
140 boulders on local sediment transport are poorly understood due to local feedbacks between
141 hydraulics and bed response (Monsalve & Yager, 2017; Nitsche et al., 2012; Yager et al., 2007).
142 Finer sediment patches commonly form on the lee side of protruding clasts due to flow
143 separation (Thompson, 2008), which in turn alter local roughness, affecting hydraulics and thus
144 sediment transport around boulders (Laronne et al., 2001). However, in boulder-bed channels
145 with low relative submergence (h/D <3.5, where h is the flow depth and D is the boulder
146 diameter; Papanicolaou & Kramer 2005), experimental studies have documented deposition of
147 fine to medium-sized sediment directly upstream of boulders (Monsalve & Yager, 2017;
148 Papanicolaou et al., 2018). Monsalve and Yager (2017) explained the formation of upstream
149 patches as a consequence of negative shear stress divergence upstream of boulders and an
150 increase in dimensionless shear stress downstream of boulders in channels with low relative
151 submergence (LRS); however, this study used a simplified system with regularly spaced equi-
152 sized hemispheres, spaced so that wakes between consecutive boulders did not interfere with one
153 another. Furthermore, the presence of protruding boulders can absorb a significant amount of
154 shear stress so that the available shear stress for entrainment and transport of mobile sediment
155 decreases, leading to potential overestimation of sediment transport (Papanicolaou et al., 2012;
156 Yager et al., 2007, 2012).

157   On a larger spatial and longer temporal scale than sediment deposition dynamics,
158 processes that drive bedform development and steer which flow is channel-forming may differ
159 for semi-alluvial and alluvial channels. In steep, gravel-bed alluvial channels, bed slope can
160 predict either a unique bedform or multiple stable states (Palucis & Lamb, 2017). For example,
161 according to Montgomery & Buffington (1997), step-pool channels commonly have slopes
162 ranging from 0.03 to 0.065 m/m; however, further studies have shown that only individual steps
163 form at slopes around 0.04 m/m and continuous steps require slopes exceeding 0.07 m/m
164 (Church & Zimmerman, 2007). At lower slopes, stone lines or transverse ribs form out of
165 cobbles and boulders, without channel-spanning pools; however, these are commonly submerged

166 even at moderate flows (Church & Zimmerman, 2007). The formation of step-pools is a
167 combination of the random location of keystones, at which other large grains come to rest
168 (Curran & Wilcock, 2005; Lee & Ferguson 2002; Zimmerman & Church, 2001), and hydraulics,
169 where step-pools form under antidune crests at high discharges so that scour occurs on the falling
170 limb creating a pool between coarser deposits (Grant, 1997; Lenzi, 2001; Whittaker & Jaeggi,
171 1982). Based on these step-forming hypotheses, the limiting factor for forming steps in boulder-
172 bed semi-alluvial channels will not be keystone clasts but rather the ability for additional large
173 grains to deposit upstream of keystones and for sufficient scour to take place downstream of
174 keystones.

175   Furthermore, regardless of whether step-pools or any other bedform or regular sediment
176 cluster can form, there is the question of which flow creates and then maintains the current
177 channel configuration, in terms of bedforms and boulder configuration. It is debated whether the
178 effective discharge, defined as the flow that transports the most sediment over time, is also the
179 discharge that determines the channel morphology (Andrews, 1980; Emmet & Wolman, 2001;
180 Lenzi et al., 2006a; Torizzo & Pitlick, 2004). Although effective discharge originally referred to
181 transport of suspended sediment (Wolman & Miller, 1960), this concept has also been applied to
182 bedload transport (e.g., Lenzi et al., 2006a; Torizzo & Pitlick, 2004). In many alluvial channels,
183 the bankfull flow, with a 1.5-2 year recurrence interval, does the most geomorphic work and is
184 the flow to which the channel has adjusted (Andrews, 1980; Phillips and Jerolmack, 2016).
185 However, depending on the system, the effective discharge for bedload may be discordant with
186 the channel-forming flow (e.g., Downs et al., 2016) and may instead be a channel-maintaining
187 discharge, while a more infrequent flow shapes the channel (Lenzi et al., 2006a). For example, in
188 alluvial, snowmelt-dominated Rocky Mountain streams, the effective discharge reflects rare
189 events (e.g., Q_{50}) in plane-bed channels, whereas the effective discharge is nearer the Q_{bf} flow in
190 step-pool channels (Bunte et al., 2014); however, the channel-forming discharge for step-pool
191 channels often reflects a higher recurrence-interval flow (Lenzi et al., 2006b). Similarly, in a
192 study in formerly glaciated mountain streams of British Columbia, the effective discharge was
193 overall very frequent but was also highly variable, depending on the threshold for gravel-sized
194 sediment transport (Hassan et al., 2014). Three stream types were observed in British Columbia
195 based on whether there was mobile or immobile gravel or whether sand was transported over
196 gravel. Channels with mobile gravel exceeded the effective discharge multiple days per year,
197 channels with immobile gravel had very low-frequency, high-magnitude effective discharges,
198 and those with mobile sand but immobile gravel showed a bimodal effective discharge.
199 Therefore, there may be a low effective discharge that does not, however, equal the channel-
200 forming discharge. In addition, the presence of large boulders and thus low relative submergence
201 increases the flow resistance (Bathurst, 2002). For example, the most accurate equations to
202 predict the grain component of flow resistance require the D_{84} in addition to D_{50} (Bray, 1979;
203 David et al., 2011; Hey, 1979). Thus the available shear stress to mobilize sediment is reduced
204 (Yager et al. 2007). Therefore the potential of flows to transport sediment decreases which
205 should increase the channel-maintaining or channel-forming discharge.
206
207   Predictions of potential sediment transport and channel re-working depend not only on
208 shear stresses associated with different flow magnitudes, but the flow history since a channel-
209 reworking flow (Masteller et al., 2019). During low-magnitude flows, sediment is locally
210 rearranged and particle interlocking increases, thus increasing the critical shear stress for particle
211 movement (Reid et al., 1985). However, during high-magnitude flow events, particle

212 interlocking is disrupted and the critical shear stress decreases, allowing for much higher
213 transport rates (Turowski et al., 2009; Masteller et al., 2019). Thus, the probability of sediment
214 transport depends on prior flows, including the time since a high-magnitude, sediment
215 transporting flow (Masteller et al., 2019; Yager et al., 2012), which may thus account for a large
216 portion of the variability in dimensionless shear stress values (Johnson, 2016). Therefore, when
217 determining whether a flow is capable of re-working the channel, the probability of a high flow
218 reworking the channel decreases if a channel has experienced previous low or medium flows. So,
219 a more conservative estimate of a channel-forming flow should be based on a channel where the
220 sediment has been locally rearranged with particle interlocking thus exhibiting a critical shear
221 stress on the higher end within the range of variability.

222 ## 1.3   Objectives

223 In order to gain insight of the morphodynamics of semi-alluvial boulder-bed channels
224 (known as 'rapids' in northern Sweden) and potential evolution of bedforms or self-organization
225 of sediment over time with multiple high flows, a flume study was designed and carried out to
226 mimic conditions in previously field studied semi-alluvial rapids in northern Sweden (Polvi et
227 al., 2014). The objective of this study was to model the development of semi-alluvial channels
228 with coarse glacial legacy sediment using a range of flows (Q_1-Q_{50}) in a flume at two different
229 slopes (0.02 and 0.05 m/m). I aimed to answer the following questions: (1) given a history of
230 potentially stabilizing, low flows, can we determine the potential range of channel-forming
231 discharges? Specifically, is a large-magnitude flow (e.g., Q_{50}) capable of reworking the channel,
232 transporting boulders and creating bedforms? Here, I define channel-forming discharge as a flow
233 that can transport boulders and re-organize potential bedforms or sediment clusters. This
234 question is addressed through observations of potential boulder transport and by calculating the
235 event-based and cumulative geomorphic work by each flow given a specific order of flows.
236 Whether or not the geomorphic work during the Q_{50} flow exceeds that of the Q_1 or Q_2 flows will
237 determine whether that higher flow is capable of re-organizing the bed. (2) Do patterns of
238 sediment erosion and deposition form around large, potentially immobile boulders? This builds
239 on the literature of boulder-bed channels in low relative submergence regime systems. These
240 results will provide management recommendations on how to best restore these semi-alluvial
241 channels in a self-sustaining manner.

242 ## 1.4 Prototype description

243 The flume study modeled semi-alluvial boulder-bed stream channels found in tributaries
244 to the free-flowing Vindel River, which with a drainage area of ~12,500 km^2 is the largest
245 tributary to the Ume River that flows into the Baltic Sea from the Scandes Mountains at the
246 Swedish-Norwegian border. From the mid-1800s to the 1970s, the stream networks were used as
247 a transport system for timber from the inland forests to the coastal sawmills, and thus nearly all
248 semi-alluvial channels were channelized. Channelization involved manual clearing of coarse
249 sediment, closing off side channels, building levees with coarse sediment (cobbles and boulders),
250 and later using bulldozers to clear the middle of the channel. Restoration started in the 1990s
251 with 'basic restoration' that entailed returning coarse sediment from levees to the main channel
252 and opening up some side channels (Gardeström et al., 2013). In 2010, 'enhanced restoration'
253 commenced that involved significantly widening the channel and obtaining large boulders (>1
254 m) from the surrounding forest that were placed into the channel in addition to the cobbles and

255 boulders that remained along the channel edge (Gardeström et al., 2013). Although virtually all
256 semi-alluvial rapids were channelized, some unimpacted reaches remain but most of them are
257 steeper than those that were channelized and subsequently restored (Polvi et al., 2014).

258   In this study, two prototype channels were used, representing enhanced restored reaches
259 (note: enhanced restored reaches are referred to as 'demo restored' reaches in Polvi et al., 2014)
260 and unimpacted reaches (Figure 1). Channel geometry and sediment distribution parameters were
261 obtained from four unimpacted and five enhanced restored stream reaches described in more
262 detail in Polvi et al. (2014). The average channel bed slope of the enhanced restored reaches was
263 ~0.02 m/m (range: 0.015-0.037 m/m), whereas unimpacted reaches had an average slope of
264 ~0.05 m/m (range: 0.029-0.074 m/m). The remainder of the channel geometry parameters,
265 including width, depth and sediment distribution, was similar between the two groups of reaches
266 (Polvi et al., 2014); channel widths range from 7-20 m and average bankfull depths are 0.5-1 m.
267 The catchments, which vary in drainage area from 9-151 km^2, consist of an average of 2.53%
268 lakes (0.04-6.65%), all of which are connected to the stream network, and an average of 21%
269 wetlands (6.00-52.40%) (SMHI, 2015). Sediment distributions were obtained from 300-particle
270 pebble counts of the nine reaches. The average median grain size was 245 mm (range: 130-400
271 mm), average 84th percentile sediment size was 624 mm, and average maximum sediment size
272 was 1670 mm (range: 1400-5000 mm). There was less than 10% sand, and examination of the
273 sub-surface sediment did not reveal higher percentages of sand; i.e., there is not substantial
274 armoring that shields a buried sand layer. This is further supported by the low rates of
275 weathering and sediment production in the region, as suggested by global-scale sediment yield
276 maps (Lvovich et al., 1991; Walling & Webb, 1983) and quantification of annual sediment flux
277 in a nearby catchment of only ~55 t/km^2 (Polvi et al., 2020), which is due to the relatively low
278 relief, crystalline bedrock (and till) and cold climate. Because of the segmented channel network,
279 where mainstem lakes are abundant, there is probably very little sediment transport of fine grain
280 sizes from upstream high-gradient reaches (Arp et al., 2007).

281   The flow regime in northern Sweden is dominated by snowmelt-runoff high flows in the
282 spring/early summer. The average annual precipitation is 600 mm, of which 40% falls as snow
283 (SMHI, 2017). The numerous mainstem lakes serve to buffer high flows, therefore low-
284 recurrence interval floods do not substantially increase in magnitude compared to higher-
285 recurrence interval floods, as seen in ratios of recurrence interval flows (Bergstrand et al., 2014).
286 For example, the Q_{50} flow is less than twice that of the Q_2 flow ($Q_{50}/Q_2 = 1.8$), and even the
287 predicted Q_{100} and Q_{500} flows are only 1.12 and 1.4 times that of the Q_{50} flow, respectively
288 (Figure S1). Ice forms in most of these channels during winter, as either surface or anchor ice
289 and flooding due to ice cover and ice jamming is also common (Lind et al., 2016). Although
290 there are few studies studying the role of ice formation and break-up on sediment transport,
291 Lotsari et al. (2015) found that boulders (up to 2 m in diameter) embedded in ice can be
292 transported downstream during ice break-up. Polvi et al. (2020) quantified the amount of
293 sediment transport under ice and during ice break-up as ~5% of annual sediment yield. However,
294 the potential effect of ice varies within a catchment, as no anchor ice forms and little surface ice
295 forms in reaches close to an upstream lake (Lind et al., 2016).

296

297   **2 Methods**

298   2.1 Flume setup

299   A mobile-bed physical model of the semi-alluvial prototype streams in northern Sweden
300   was set up in an 8-m long, 1.1-m wide fixed-bed flume at the Colorado State University
301   Engineering Research Center in Fort Collins, Colorado, USA (Figure 2). Using a geometric (y_r
302   and z_r) scaling factor of 8, the initial sediment distribution was scaled-down to be analogous to
303   that in the semi-alluvial prototype streams, and because the flume D_{10} was 4 mm and D_{min} was
304   0.14 mm, all sizes were sand-sized or above so there were no issues with cohesiveness (Table 1).
305   No sediment feed was provided from upstream, creating clear water conditions, and this is
306   consistent with the prototype field conditions with very low levels of suspended sediment or
307   annual sediment flux (Polvi et al., 2020) and little sediment input from the hillslopes or upstream
308   reaches. Two flume setups were used with initial bed slopes of 0.02 and 0.05 m/m, respectively.
309   Before the flows were run, the grain size distribution was thoroughly mixed in the flume, and
310   checks were made to ensure equal sediment depth and the desired slope throughout the flume
311   length. For each slope, four runs were conducted with flows analogous to the summer high (Q_1),
312   the 2-year (Q_2), 10-year (Q_{10}), and 50-year (Q_{50}) flows in the prototype streams. The summer
313   high flow (Q_1) was not based on a bankfull flow that filled the banks in the flume channel, but
314   rather based on field conditions in the prototype channels. Flow measurements were taken in the
315   field at the summer high flow, which was close to or just below the geomorphically-defined
316   bankfull flow (Gardeström J.*, unpublished data*) (see Section 2.2. for a full description of flows).
317   Each flow was run for 60 minutes, which surpassed the time necessary until equilibrium
318   conditions were met, as defined by minimal to no visible sediment transport or transport out of
319   the reach. As no boulder ($>D_{84}$) movement was detected (other than slight rotation, as described
320   in Results) during any flow, equilibrium conditions were only based on transport of the fine
321   sediment fraction. After each flow, the bed topography and channel geometry were measured
322   (described below in Section 2.3) before running the next higher flow. After the flume's slope
323   was changed from 0.02 to 0.05 m/m, sediment lost from the previous slope setup was returned
324   and all sediment was manually mixed with shovels, so that the initial conditions for both slopes
325   had a plane bed with well-mixed sediment sizes. This experimental setup means that initial
326   conditions were different for the two slopes and for each flow. However, due to the wide
327   sediment size distribution, it would be nearly impossible to replicate initial conditions for each
328   flow and slope. Therefore, the results should not be used to compare processes between slopes
329   but to be used as two case studies of boulder-bed semi-alluvial reaches. The bed degraded
330   slightly during each subsequent flow, as seen through an increase in slope: for the 2% slope
331   setup, the centerline slope started at 0.022 m/m and changed to 0.0211, 0.0223, 0.0226, and
332   0.0222 m/m with each consecutively higher flow; for the 5% slope setup, the centerline slope
333   started at 0.0532 m/m and changed to 0.0538, 0.0538, 0.0549, and 0.0545 with each
334   consecutively higher flow. However, this reach-scale degradation is fairly minor in terms of
335   changing initial conditions for each flow, and the centerline slope was controlled more by local
336   sediment re-arrangement rather than reach-scale degradation. With this setup, channel width
337   could not adjust; however, due to the coarse sediment sizes, it is assumed that adjustment of the
338   channel would occur via downstream sediment transport rather than streambank erosion and
339   lateral migration.

340

341

342
343 **Figure 2.** Photos of each flume run at two slope setups with four different flow magnitudes.
344 Pictures a-d were taken at the 2% slope setup, and pictures e-h were taken at the 5% slope setup.
345 Photos a & e were taken at Q_1 (0.006 m^3/s); photos b & f at Q_2 (0.017 m^3/s); photos c & g at Q_{10}
346 (0.025 m^3/s); and photos d & h at Q_{50} (0.031 m^3/s).

347

348

349

350   **Table 1.** Prototype Reach Characteristics and Corresponding Flume Specifications

	Prototype reach characteristics	**Flume specifications**
Bed Slope	Restored channels: 0.8-3.7%	Setup 1: 2%
	Unimpacted channels: 2.9-7.4%	Setup 2: 5%
Width	8.8 m	1.1 m
Length	64.0 m	8.0 m
Sediment Input	Crystalline rocks, low levels of weathering, and abundant lakes that buffer sediment = low levels of suspended sediment	Clear water (no sediment feed)
Initial Conditions	Rapids form in poorly sorted till within moraines and eskers	Unsorted sediment mix, with plane bed morphology
Sediment size distribution		
D_{16}	56 mm	7 mm
D_{50}	248 mm	31 mm
D_{84}	624 mm	78 mm
D_{max}	1672 mm	209 mm
Flows & unit discharges		
Q_1	1.0 m^3/s / 0. 125 m^2/s	0.006 m^3/s / 0.005 m^2/s
Q_2	3.1 m^3/s / 0. 062 m^2/s	0.017 m^3/s / 0.015 m^2/s
Q_{10}	4.6 m^3/s / 0.577 m^2/s	0.025 m^3/s / 0.023 m^2/s
Q_{50}	5.6 m^3/s / 0.705 m^2/s	0.031 m^3/s/ 0.028 m^2/s

351

352   2.2 Flume flows

353   For each of the four unimpacted and five enhanced restored stream reaches studied in
354   Polvi et al. (2014), the various flow magnitudes that represent the Q_2, Q_{10} and Q_{50} flows were
355   derived from a hydrological model, S-HYPE, developed by the Swedish Meteorological and
356   Hydrological Institute S-HYPE (Lindström et al., 2007; SMHI, 2015). The average of each of
357   these flows for the nine reaches were used to calculate the desired discharge for the flume runs.
358   The Q_1 flow magnitude was based on high flow field-measurements of enhanced restored
359   streams (Gardeström J., *personal communication*); although this may not equate to a flume
360   channel-filling flow, it is analogous to the flow magnitude experienced by the prototype channel
361   most years directly after the snowmelt-induced spring flood. The experimental flows were scaled
362   down by a factor of 181.02 according to equation (1) following Froude number similitude over
363   fixed beds (Julien, 2002). Although the objective of this study was to model temporal evolution
364   of the bed and potential bedforms, scale effects used for mobile bed Froude models was not
365   deemed to play a significant role. Because the main objective of scaling the discharge was to
366   obtain relative changes in flow that correspond to different recurrence intervals in the field, exact
367   correspondence to a specific flow was not necessary. Also in Froude scaling, non-dimensional
368   shear stress scales directly, thus entrainment of model particles will be equal to that in the field.
369   For each flume setup, a low-flow discharge was run first to provide saturated conditions prior to
370   the experimental runs. Discharge was measured in a closed pipe prior to the inflow in the flume
371   using a Badger-meter M2000 flow meter. Before entering the flume, the inflow was allowed to

372 mix in a 'crash box' for ~0.5 m to dampen turbulence before entering the flume. The top 0.5 m
373 of the flume was lined with very coarse sediment so that preferential scour and sediment
374 entrainment did not occur where the water first entered the flume over a lip. Morphologic
375 measurements started downstream of the coarse sediment buffer zone. Likewise, at the
376 downstream end of the flume, sediment was preferentially transported as a headcut formed.
377 However, the morphologic analyses were cut off where this effect was seen.

378 $$Q_r = y_r z_r{}^{3/2} \tag{1}$$

379 2.3 Morphologic & hydraulic data acquisition and analyses

380   Structure-from-motion photogrammetry (SfM) was used to create digital elevation
381 models (DEMs) of bed topography (Westoby et al., 2012). SfM-created DEMs were constructed
382 before all runs at each slope setup and after each run, with progressively higher flows. For each
383 flume setup with different slopes, a terrestrial LiDAR scan (TLS) was used to determine a
384 coordinate system and be able to georeference the SfM scans, based on targets affixed to the
385 flume walls. The TLS scans provided exact xyz coordinates of the targets, which were used to
386 georeference the SfM-based DEMs. A Canon EOS Rebel T3i DSLR camera with a fixed, non-
387 zoom lens (Canon EF-S 24 mm prime lens), which minimizes edge distortion of photos, was
388 mounted to a movable cart on rails ~30 cm above the flume bed. Photos were taken ~20 cm apart
389 looking upstream and downstream at an oblique 45° angle. This flume setup and sediment
390 distribution was included in a study comparing results from SfM and TLS scans, which found
391 that SfM can produce topographic point clouds with comparable quality and greater point
392 densities to TLS (Morgan et al., 2017), thus verifying the validity of the SfM scans in this study.
393 The images were processed using AgiSoft PhotoScan Professional (Agisoft LLC, 2014) to obtain
394 topographical point clouds.

395   The topographical point clouds were imported into ArcMap 10.5.1 (ESRI, 2017) and
396 rasters were created with a grid size of 5 mm to create digital elevation models (DEMs) of the
397 topography for the initial conditions at each slope setup and after each flow with a precision of 2
398 mm (Polvi, 2020; Figure 3). In areas with missing data, the neighboring points were iteratively
399 averaged to interpolate elevations for pixels. The flume study area was clipped to 7.0 m and 6.3
400 m in length for the 2% and 5% slope setups, respectively, to remove the upstream turbulent
401 section containing much coarser sediment and a headcutting section at the downstream portion of
402 the flume. To analyze differences in aggradation versus degradation after each run, the DEMs
403 were subtracted from one another to create DEMs of difference (DoDs) (Wheaton et al., 2010);
404 DoDs were created comparing each flow to the initial conditions and after each successive flow.
405 In addition, all large clasts, defined as sediment clasts $>D_{84}$ (~80 mm in diameter), were digitized
406 (Polvi 2020), and the spatial distribution of aggradation and degradation in relation to the large
407 clasts were analyzed by creating buffers equal to half the diameter of the respective clasts. Each
408 buffer was then split into an upstream and downstream half, and the mean elevation change in
409 each upstream and downstream buffer was calculated using zonal statistics within ArcGIS. One-
410 sample t-tests were used to determine whether the mean elevation change in all of the upstream
411 and downstream buffers after a given flow, compared to the previous flow and compared to the
412 pre-flow conditions, were significantly different from 0. Two-sample t-tests were used to
413 determine whether the mean elevation change differed between the upstream and downstream
414 buffers for a given flow compared to the previous flow and compared to the initial conditions.

415   Although some downstream buffers were close to or slightly overlapped with an upstream buffer
416   for another clast, or vice versa, the effect of other large clasts in the vicinity of a buffer may
417   contribute to variation in the mean values but should not affect the overall mean values. All
418   statistical analyses were performed using the statistical software 'R' (RStudio Team, 2016).

419   The total geomorphic work done by each flow was calculated as the sum of the volume of
420   aggradation and degradation in the entire flume area, which is different than the standard method
421   of using transport rates and assumes that large channel changes implies relatively high transport
422   rates. Because the flows were run in order from lowest to highest for each slope setup, the
423   geomorphic work for the higher flows may be underestimated due to interlocking of grains
424   during lower flows (e.g., Masteller et al., 2019); therefore, the geomorphic work for each flow is
425   also reported as the cumulative combined aggradation and degradation of that flow in addition to
426   all prior flows. To determine how much the sediment was reworked after each flow, the percent
427   of the flume area that experienced erosion or deposition was calculated by determining how
428   many pixels (5 mm x 5 mm) in DoDs experienced >0.01 m or < -0.01 m of elevation change and
429   by transforming this to a percent of the entire bed. Thresholding of the DoDs was only done for
430   visualization purposes (Figures 4a, S2, S3) and for calculation of the area affected by erosion or
431   deposition (>0.01 m of elevation change). For the volume analysis of erosion/deposition,
432   potential errors would contribute to negligible or small volumes compared to actual change. For
433   the D_{84} buffer analysis, random errors should cancel each other out (positive and negative
434   change) in calculation of mean elevation change. DEMs were detrended to visualize topography
435   throughout the entire reach (Figure 3). Using the detrended DEMs, topographical roughness was
436   calculated as the standard deviation of elevation values.

437   Because the main objective of this flume experiment was to analyze changes in
438   morphology, detailed hydraulic measurements were not made. However, flow depths were
439   recorded longitudinally spaced throughout the channel and at three lateral locations during each
440   flow. Missing flow depth data from the first two flows at the 2% slope setup were estimated
441   using time-lapse photos during the runs and DEMs by measuring flow depths based on the water
442   surface elevation. Reach-scale averages of flow depth were used to calculate the reach-averaged
443   shear stress (Equation 2), relative submergence, and Froude number. The maximum potentially
444   entrained sediment size was calculated for each flow using Shield's equation (Equation 3), using
445   the traditional critical dimensionless shear stress (τ_c^*) value of 0.045 and a higher value of 0.1,
446   which may be more accurate for steep streams (Lenzi et al., 2006b).

447    $\tau = \rho_w g h S$ (2)

448   where, τ is the reach-scale shear stress (N/m^2), ρ_w is the density of water (1000 kg/m^3), g is
449   acceleration due to gravity (9.81 m/s^2), h is the average flow depth, and S is the reach-averaged
450   bed slope.

451    $D = \dfrac{\tau}{\tau_c^*(\rho_s - \rho_w)g}$ (3)

452   where, D is the maximum mobile sediment size (m), τ is the reach-scale shear stress (N/m^2), τ_c^*
453   is the dimensionless critical shear stress, ρ_s is the density of sediment (2650 kg/m^3), ρ_w is the
454   density of water (1000 kg/m^3), and g is acceleration due to gravity (9.81 m/s^2).

455
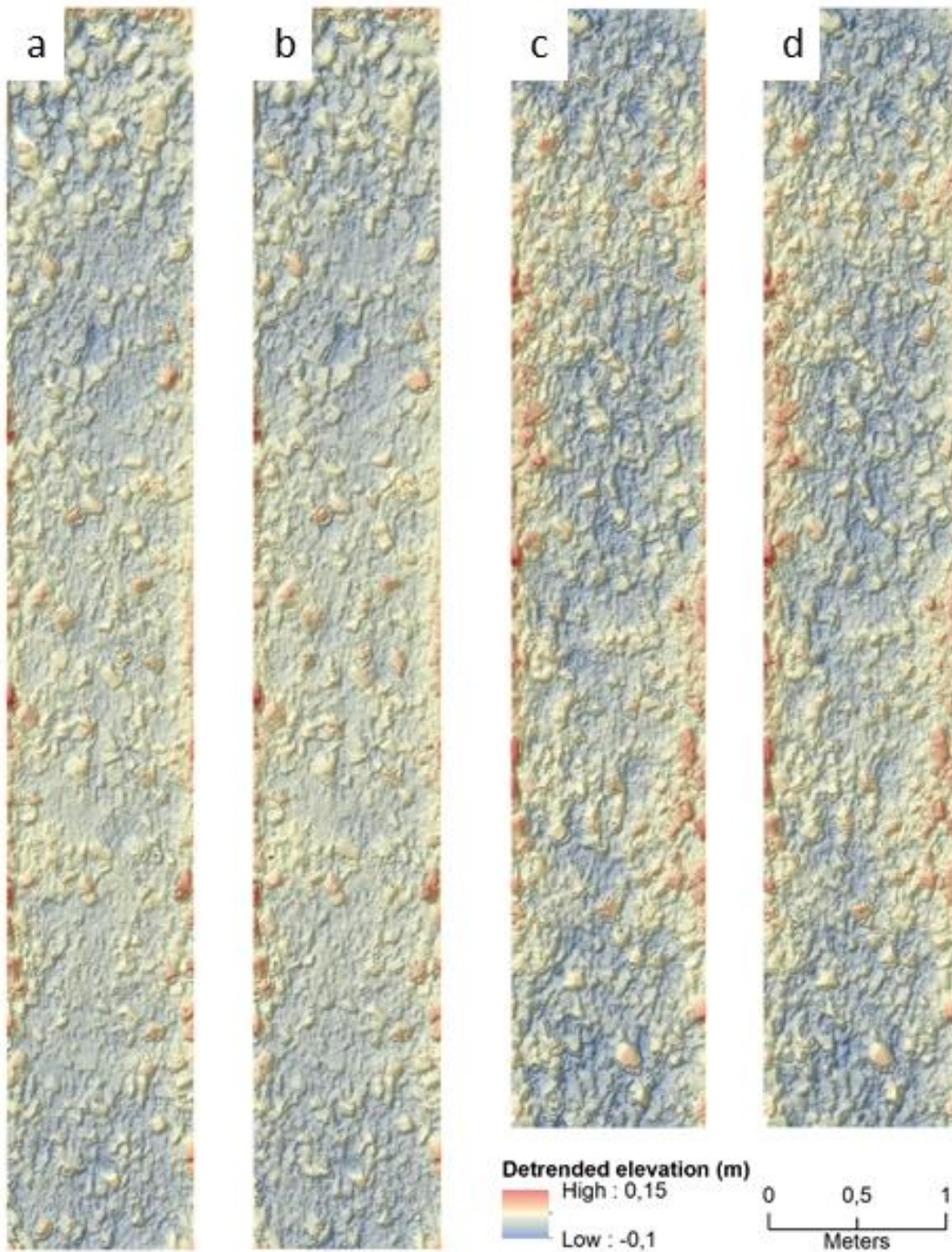
Figure 3. Detrended digital elevation models based on structure-from-motion photogrammetry at the 2% slope setup (a & b) and 5% slope setup (c & d), showing initial conditions (a & c) and channel bed topography after the Q_{50} flow (b & d). Color scales show relative detrended elevations in meters. Distance scale bar applies to all DEMs. Note that the analyzed flume area was slightly shorter with the 5% slope setup due to the larger affected area by headcutting.

462   **3 Results**

463   3.1 General visual observations

464   At both slope setups, the large clasts ($>D_{84}$) were basically immobile, with some
465   downstream rotation and imbrication observed at the Q_{50} flow at the 5% slope. Medium-sized
466   sediment ($\sim D_{50}$) also showed imbrication at the Q_{10} and Q_{50} flows at both slopes; imbrication
467   was located directly upstream of large clasts or independent of the hydraulic influence of
468   boulders (Figure 4b; 4c). Most sediment transport occurred at the beginning of each flow, and
469   mobile sediment was quickly deposited in shielded or stable locations, inhibiting potential
470   further transport until the next higher discharge was run. Sediment clusters of small- to medium-
471   sized sediment ($\sim$4-20 mm), corresponding to grains sizes between the D_{10} and D_{50}, were
472   observed upstream of immobile clasts after the Q_{10} flows at both slope setups, with
473   corresponding scour downstream of immobile clasts (Figure 4). No boulders ($>D_{84}$) were mobile
474   during the experiment, other than very slight rotation at the highest flow (Q_{50}) at the higher slope
475   (5%) due to scour downstream of boulders. Because the large clasts remained immobile at all
476   flows, no classic bedforms, including steps, developed in these experiments; however, the
477   formation of small-scale bedforms and structures around boulders are discussed below (section
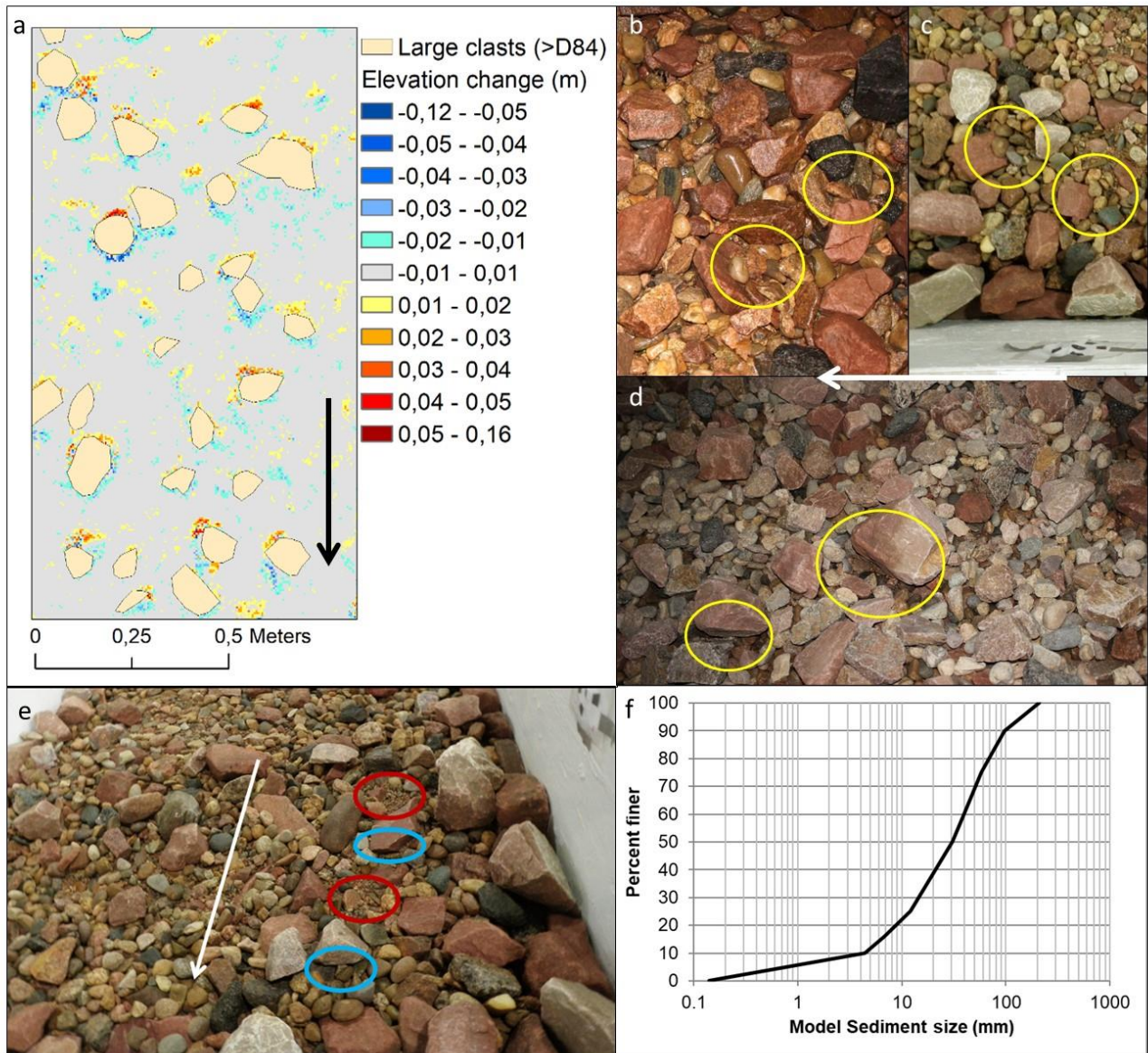478   3.3).

479
480 **Figure 4.** Patterns of erosion and sedimentation after flume runs: a) elevation change after Q_{10}
481 flow at 2% slope setup around large clasts ($>D_{84}$). Photos (b & c) show imbrication, both after
482 Q_{10} flow, at 5% and 2% slope setups, respectively. (d) Scour forms downstream of large clasts
483 after Q_{50} flow at 5% slope setup, which caused slight downstream rotation of large clasts. (e)
484 Photo after Q_{10} flow at 2% slope setup showing patterns of sedimentation (red) and scour (blue)
485 around large clasts. (f) Sediment size distribution for flume experiments. See Polvi et al. (2014)
486 for range of grain size distributions for enhanced (referred to as 'demo') and unimpacted reaches.
487 Arrows indicate flow direction.

488   The relative submergence (RS) of large boulders ($>D_{84}$) differed for each flow but were
489 similar between slope setups (Figure 2; Table 2); RS values were calculated for the D_{84} clast size
490 and is therefore lower for larger clasts. At the bankfull flow, the RS was very low (0.31 and 0.32)
491 at both slopes; a few surface waves were evident at the 5% slope but very little turbulence or
492 surface waves were evident at the 2% slope. At Q_2, wakes start to form downstream of boulders,

493   and the RS was ~0.6. The RS at the Q_{10} flow was approaching 1 at the 2% slope (0.87 for D_{84})
494   and ranged from ~0.8-1.2 for the 5% slope with clear boulder-affected wakes forming. At the Q_{50}
495   flow, all boulders were nearly submerged at both slopes. At the 2% slope, the RS = 1.0 and
496   waves and wakes formed downstream of boulders; at the 5% slope, the average RS was
497   calculated to be less than 1 but according to visual observations seemed to range from 1-1.5 with
498   very turbulent flow. All reach-scale Froude numbers were below 1 (Table 2), but there was
499   variation throughout the reach with local zones of critical and supercritical flow around clasts
500   $>D_{84}$, particularly at Q_{10} and Q_{50} flows.

501   3.2 Summary of aggradation/degradation results

502   Less than 20% (7.13- 19.91%) of the flume area was re-worked through erosion or
503   deposition (>0.01 m positive or negative elevation change) during each flow for both slope
504   setups (Table 3). At the 2% slope, 3.40-9.80% of the flume area was eroded after each flow, and
505   1.58-7.60% of the flume area experienced deposition. At the 5% slope, 4.93-10.39% of the flume
506   was eroded, and 5.85-11.26% of the flume area experienced deposition.

507   At the 2% slope, the Q_{10} flow does the most amount of work (0.044 m^3), followed closely
508   by the Q_1 flow (0.042 m^3) (Table 3). This was visually observed during the flume runs as the
509   bankfull flow was able to mobilize fine sediment. Because there was no input of fine sediment
510   during or between the runs at a given slope, by the time the highest flow (Q_{50}) was run, all
511   potentially mobilized sediment had either already been transported out of the system or settled
512   into a shielded or non-mobile position. With little available fine sediment, combined with the Q_{50}
513   flow not being competent enough to start mobilizing the large clasts ($>D_{84}$), the largest flow, Q_{50},
514   actually does the least amount of work (0.028 m^3). Because it would not have been possible to
515   re-create the exact same initial conditions with such a wide grain size distribution (Figure 4f), the
516   closest estimation of comparing the work by each flow from initial conditions is by calculating
517   cumulative geomorphic work. Here, the Q_{50} flow eroded and deposited ~3.5 times as much
518   sediment as the Q_1 flow but only 1.2 times that of the Q_{10} flow (Table 3).

519   At the 5% slope, the Q_{50} flow does the most amount of geomorphic work (as measured
520   by the total aggradation and degradation), followed in descending order by the Q_1, Q_2, and Q_{10}
521   flows. As noted by visual observations of the flume runs and the DoDs, at the Q_{50} flow, the
522   largest clasts start to mobilize by rolling slightly (due to downstream scour); but the other flows
523   show the same process as with the 2% slope, where the potentially mobile sediment has already
524   been moved. Considering cumulative geomorphic work, the Q_{50} flow eroded and deposited ~3.5
525   times as much sediment as the Q_1 flow and 1.6 times that of the Q_{10} flow at the 5% slope (Table
526   3).

527   The shear stress for the Q_1 flow at the 5% slope was roughly the same as that of the Q_{10}
528   flow at the 2% slope. At the Q_2 flow at the 5% slope, the shear stress (22.3 N/m^2) already
529   exceeded that of the stream power at the Q_{50} flow at the 2% slope (13.36 N/ m^2); however, the
530   geomorphic work do not differ greatly between slopes for the same slopes, likely because shear
531   stresses were not sufficient to entrain the coarser fractions even at the 5% slope (Table 2). Based
532   on a conservative τ_c^* of 0.1, the shear stress at the Q_{50} flow at the 2% slope is predicted to
533   entrain a maximum sediment size of 9.4 mm, which is only slightly larger than that of the D_{16}
534   sediment size. The same analysis for the Q_{50} flow at the 5% slope predicts entrainment of a

535 maximum sediment size of 20.2 mm, which is slightly less than that of the D_{50} grain size (Table
536 2).

Table 2. Hydraulic & Shear Stress Parameters

Slope	Flow	Q (m³/s)	Stream power Ω (N/s)	Froude #	Average flow depths (m)	Relative submergence (d/D84)	τ (N/m²)	Mobile sediment threshold (m) (τ*$_c$ = 0.045)	Mobile sediment threshold (m) (τ*$_c$ = 0.1)
2%	Q$_{bf}$	0.006	1.18	0.47	0.024	0.31	4.48	0.006	0.003
	Q$_2$	0.017	3.34	0.45	0.049	0.63	8.87	0.013	0.006
	Q$_{10}$	0.025	4.91	0.41	0.068	0.87	11.83	0.018	0.008
	Q$_{50}$	0.031	6.08	0.42	0.078	1.00	13.36	0.021	0.009
5%	Q$_{bf}$	0.006	2.94	0.43	0.025	0.32	11.88	0.017	0.008
	Q$_2$	0.017	8.34	0.45	0.050	0.64	22.30	0.033	0.015
	Q$_{10}$	0.025	12.26	0.51	0.058	0.75	25.91	0.039	0.018
	Q$_{50}$	0.031	15.21	0.52	0.067	0.856	29.20	0.045	0.020

538
539
540
541 **Table 3.** Erosion, deposition and geomorphic work calculations
542
543

Slope	Pre-flow	Flow	Q (m³/s)	Std. Dev. DEM (m)	Flume area with deposition (%)[a]	Flume area with erosion (%)[a]	Flume area with erosion or deposition (%)[a]	Volume of aggradation (m³)	Volume of degradation (m³)	Geomorphic work (m³)[b]	Cumulative geomorphic work (m³)[c]	Cumulative work per area (m)
2%		Pre		0.0228								
	Pre	Q$_1$	0.006	0.0231	4.83	9.80	14.63	0.013	-0.029	0.042	0.042	0.006
	Q$_1$	Q$_2$	0.017	0.0228	1.58	5.55	7.13	0.019	-0.017	0.036	0.079	0.011
	Q$_2$	Q$_{10}$	0.025	0.0229	7.60	7.91	15.51	0.022	-0.021	0.044	0.122	0.017
	Q$_{10}$	Q$_{50}$	0.031	0.0228	4.32	3.40	7.73	0.015	-0.013	0.028	0.150	0.021
5%		Pre		0.0304								
	Pre	Q$_1$	0.006	0.0308	5.85	7.07	12.92	0.017	-0.020	0.037	0.037	0.005
	Q$_1$	Q$_2$	0.017	0.0307	6.08	4.93	11.01	0.019	-0.015	0.034	0.071	0.010
	Q$_2$	Q$_{10}$	0.025	0.0306	11.26	7.48	18.74	0.006	-0.003	0.010	0.080	0.012
	Q$_{10}$	Q$_{50}$	0.031	0.0303	9.52	10.39	19.92	0.024	-0.027	0.050	0.131	0.019

[a] % area of deposition and erosion defined as area that experienced > 0.01 m net positive or negative elevation change.

[b] Geomorphic work is defined as the cumulative sum of absolute values of aggradation and degradation after each flow.

544 [c] Cumulative geomorphic work is defined as the sum for the given flow with all previous flows.

545 3.3 Erosion and deposition next to large clasts

546   Statistically significant differences in the mean elevation change of upstream and
547 downstream buffers around large clasts (>D_{84}) were found at both slope setups, and similar
548 trends were observed between each of the flows at both slopes, indicating patterns of sediment
549 organization in relation to large immobile clasts (Figure 4 & 5). After the Q_1 flow, significant
550 degradation occurred in both the downstream and upstream buffers at the 2% slope, whereas
551 there was only significant degradation in the downstream buffer at the 5% slope. Only the 5%
552 slope showed significant differences in the upstream and downstream buffer after Q_1, with more
553 aggradation upstream. Both slope setups showed significant differences after the Q_2 flow with
554 more aggradation in the downstream buffers, but at the 5% slope there was no significant change
555 in elevation in the upstream buffers. The Q_{10} flow showed significant upstream buffer
556 aggradation at both slopes and significant degradation in the downstream buffers at the 2% slope.

557   The opposite trend was evident at the Q_{50} flow at the 5% slope with degradation in upstream
558   buffers; at the 2% slope, significant, yet minimal, aggradation was found in both upstream and
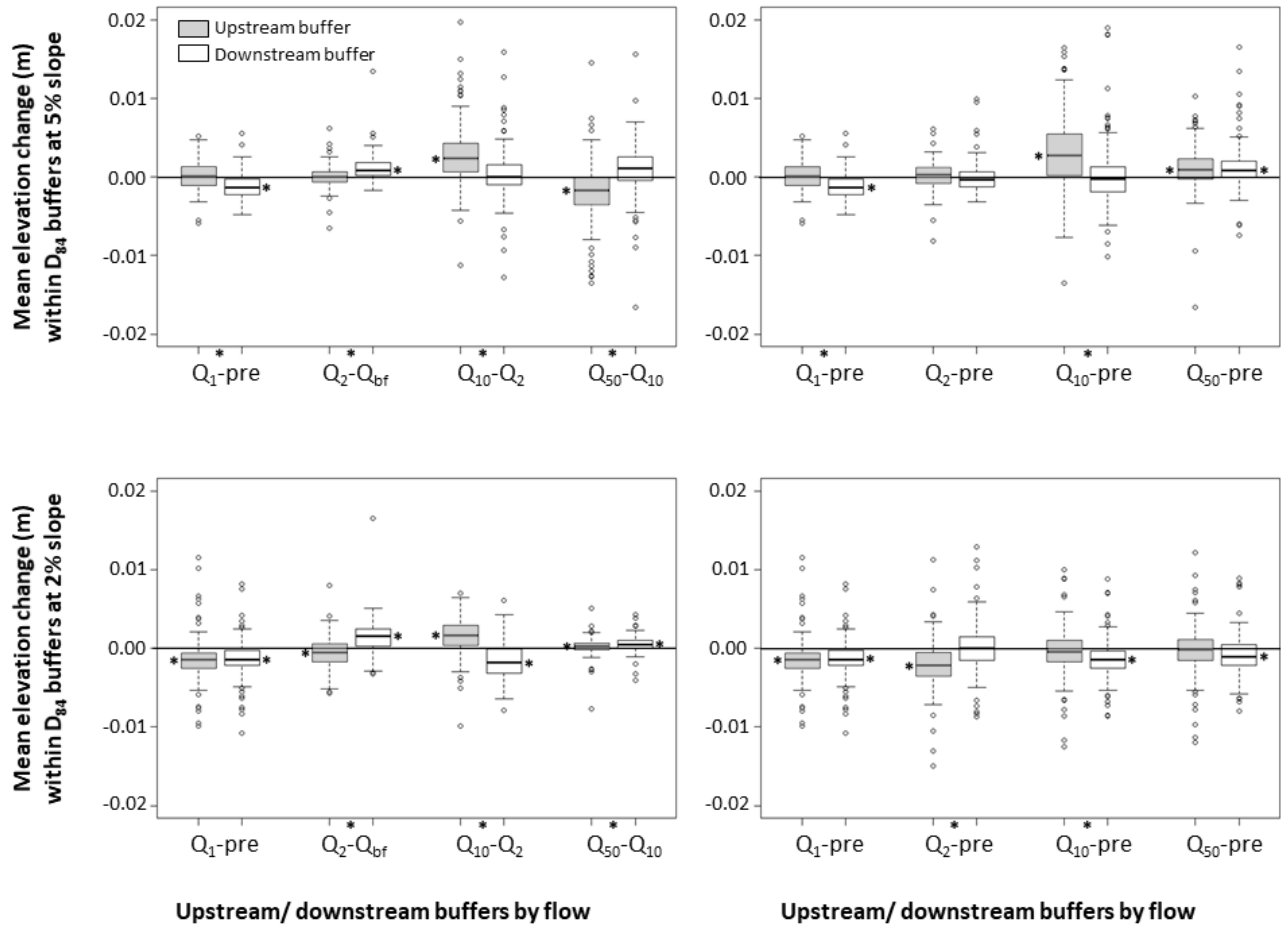559   downstream buffers.

560
561   **Figure 5.** Boxplots of mean elevation change (i.e., aggradation/degradation) in buffers upstream
562   (grey) or downstream (white) of D_{84} clasts. Boxplots on left show comparisons between previous
563   flow and boxplots on right show comparisons between each flow and pre-flow conditions.
564   Asterisks next to boxplots denote that mean is significantly different from 0 at (α=0.05) and
565   asterisks between labels on x-axis denote that there is a significant difference between the mean
566   elevation change in the upstream and downstream buffers.

567   **4 Discussion**

568   4.1 Geomorphic work and channel reworking

569   This flume experiment was designed to elucidate how semi-alluvial boulder-bed channels
570   with a snowmelt-dominated flow regime evolve in terms of potential bedforms or sediment
571   clusters. The first aspect of determining what controls channel evolution in these channels was to
572   examine which flow does the most geomorphic work and whether it is possible to determine
573   which flow is the channel-forming discharge within the present flow regime. These flows were
574   modeled with clear-water conditions, which was considered representative of what these

575   channels experience in northern Sweden due to the low sediment production in the landscape and
576   lakes along the stream network buffer sediment coming from upstream. Therefore, the order of
577   the flows, which was from the lowest to the largest flows, played a role in determining how
578   much sediment was available to be re-worked. At the 2% slope, the Q_1 flow did almost the same
579   amount of work as the Q_{10} flow (0.042 and 0.044 m^3 of combined aggradation and degradation,
580   respectively). The Q_{50} flow did the least amount of geomorphic work at the 2% slope, because
581   there was very little mobile sediment remaining after the previous lower flows had deposited the
582   available sediment in stable locations, thus potentially increasing the critical shear stress
583   (Masteller et al., 2019). Cumulative geomorphic work is naturally largest for the Q_{50} flow, as it
584   has summed aggradation and degradation for previous flows; however, the cumulative
585   geomorphic work for the Q_{50} flow is only slightly less than twice that of the Q_1 flow at the 2%
586   flow. In channels with a broad or bimodal sediment distribution, clusters tend to remain stable
587   unless the anchor sediment is entrained during high flows (Hendrick et al., 2010); therefore, once
588   sediment clusters form at lower flows, those sediment particles are more difficult to mobilize
589   even at higher flows. At the 5% slope, the Q_1 and the Q_2 flows did similar amounts of
590   geomorphic work, which was approximately three times the amount as that of the Q_{10} flow. This
591   sudden decrease in sediment transport during the Q_{10} flow can also be explained in a similar way
592   to that of the Q_{50} flow at the 2% slope, that all potentially mobile sediment had been mobilized
593   and deposited in a stable setting before the Q_{10} flow. The Q_{50} flow did almost 1.5 times the
594   amount of geomorphic work of the Q_2 and Q_{10} flows at the 5% slope, but this is an artefact of
595   slight downstream rotation of large clasts, which appears as downstream sedimentation and
596   upstream degradation relative to boulders' previous positions. However, as these results are
597   dependent on the sequencing of flows, they should not be interpreted as indicative of the relative
598   amount of geomorphic work done by these flows over a longer period of time with a varying
599   sequences of flow events. That said, these results can indicate whether the larger flows are
600   capable of resetting the channel by reworking most of the bed sediment and entraining boulders.
601   Because the Q_{50} flow did less geomorphic work than the Q_1 at the 2% slope, the Q_{50} is clearly
602   not capable of reworking the channel bed. Although the Q_{50} flow did do more geomorphic work
603   than the Q_1 flow at the 5% slope, the higher amount of work is an artefact of slight rolling of
604   large clasts and thus the Q_{50} did not rework the channel bed at the higher slope either.

605   Through this flume experiment, it was only possible to test flows up to Q_{50}, due to the
606   capacity of the pump; however, we can get a sense of the magnitude of flows necessary to
607   transport boulders and re-work the channel bed. In this experiment, the geomorphic work done
608   by the Q_{50} flow may be underestimated because it was preceded by several runs with lower flows
609   that can cause interlocking of grains, thus increasing the necessary critical dimensionless shear
610   stress (Masteller et al., 2019). However, given that the Q_{50} flow did not re-work the channel
611   more than the Q_1 flow and no clasts >D_{84} were transported, we can conclude that the Q_{50} flow is
612   not capable of disrupting grain interlocking in these channel types. In other steep, coarse-grained
613   channels, boulder or bedform reorganization occurs during much higher recurrence interval
614   flows; for example, step-pool structures in the Erlenbach (18% slope) were completely
615   rearranged three times within a 20-year period (Turowski et al., 2009). The recurrence interval of
616   the effective or channel-forming discharge in other steep gravel-bed channels have ranged from
617   the Q_1 to the Q_{50} flow depending on slope, sediment size distribution and bedforms (Bunte et al.,
618   2014; Hassan et al., 2014; Lenzi et al. 2006a). Results from this study indicate that these semi-
619   alluvial rapids are similar to step-pool channels in alluvial, snowmelt-dominated Rocky
620   Mountain streams where low flows may do a large amount of geomorphic work, depending on

621   the history of previous flows (Bunte et al., 2014; Hassan et al., 2014). However, these low flows
622   may only reflect a channel-maintaining and not a channel-forming flow (Hassan et al., 2014).

623   That begs the question of if fairly high flows (Q_{50}) are not capable of mobilizing
624   boulders, what is the channel-forming flow and how did these channels originally form? Because
625   of the snowmelt-dominated flow regime with buffering of flows by mainstem lakes, extremely
626   high flows are unlikely (Arp et al., 2006; Bergstrand et al., 2014). The Q_{50} flow is only 1.8 times
627   that of the Q_2 flow in this experiment, and the ratio of the Q_{50} to the Q_1 in this region ranges from
628   1.5-1.9 (Bergstrand et al., 2014). If the Q_{100} and Q_{500} flows follow the same logarithmic trend,
629   those flows will only be 1.12 and 1.38 times that of the Q_{50} flow, respectively. Furthermore, the
630   prototype channels are located in partly confined to unconfined moraine-, drumlin-, or esker-
631   bounded floodplains, so flow depths would not increase significantly with higher flows. There
632   are few mechanisms for post-glacial extreme flows in streams originating below the Scandes
633   mountains in inland northern Sweden. Potential mechanisms for extreme flows, which do not
634   follow the modeled RI-Q relationships, that cannot be ruled out include local cumulative effects
635   of breached beaver dams or moraine-dammed lakes combined with a rain-on-snow event over
636   seasonally-frozen ground. Based on the low magnitude of low-recurrence interval hydrologic
637   events in this region, combined with results from this study showing that the Q_{50} flow is not
638   channel-forming, it is unclear how often channel-forming flows, that are capable of transporting
639   boulders, occur in these streams.

640   Large rivers in northern Sweden (e.g., Ume, Vindel, Lule Rivers) with steep bedrock
641   gorges, to which these semi-alluvial channels are tributaries, were formed by sub-glacial
642   meltwater while glaciers were melting ca 10,000 y. BP and have experienced very little fluvial
643   erosion post-glaciation (Jansen et al., 2014). Although this study did not model higher than Q_{50}
644   flows, there is a possibility that these semi-alluvial channels have not experienced a channel-
645   forming discharge (capable of transporting boulders) since directly pre- or post-deglaciation
646   when flow magnitudes could have been much larger and under higher pressure (Herman et al.,
647   2011) and thus competent enough to move large boulders. Assuming a generous τ_c* of 0.045, a
648   flow depth of 0.29 m (3.7 times that of the Q_{50} flow depth) and a shear stress 4 times that of the
649   Q_{50} flow would be required to entrain D_{84} sediment in the flume at the 2% slope; at the 5% slope,
650   a water depth of 0.26 m (3.8 times that of the Q_{50} flow depth) and shear stress nearly double that
651   observed at the Q_{50} flow would be required. Due to the mostly unconfined to partly confined
652   nature of the prototype streams, reaching analogous mean flow depths (2.3 m and 2.1 m,
653   respectively) would require extremely high magnitude flows. However, during deglaciation
654   (~9000-10000 y BP), glaciers receded very rapidly at ~100 km in 100 years in the inland region
655   below the Scandes mountains (Lundqvist, 1986; Stroeven et al., 2016), with the rate varying
656   between 200 and 1600 m yr^{-1} in the region (Stroeven et al., 2016). This high deglaciation rate led
657   to locally high discharges: modelled summer discharges in sub-glacial tunnels at the ice margin
658   during deglaciation range from 100 to 300 m^3/s (Arnold & Sharp, 2002; Boulton et al., 2009).
659   These post-glacial discharges are two orders of magnitude greater than the current Q_{50} and the
660   extrapolated Q_{100} or Q_{500} flows and would thus be capable of transporting much larger clasts than
661   current flow regimes allow. Since then, with the current snowmelt-dominated flow regime
662   buffered by lakes, hydraulic processes provide few mechanisms for these channels to re-organize
663   in terms of steps, pools or other large bedforms.

664   Another potential mechanism for localized sediment transport, including that of boulders
665 is winter ice cover and ice break-up (Lotsari et al., 2015; Polvi et al. 2020). Although boulders
666 up to 2 m in diameter can be transported by ice during ice break-up (Lotsari et al., 2015), it is
667 unclear how important the role of sporadic, localized transport by ice is for long-term channel
668 formation (Ettema & Kempema, 2013). Therefore, channels may have inherited their overall
669 geometry from unsorted glacial sediment, yet fluvial flows and ice processes from the current
670 flow regime have likely promoted the formation of sediment clusters and control microhabitat
671 formation.

672 4.2 Bedforms and sediment clusters

673   Within the flows modelled in this flume experiment, no classic alluvial steep-channel
674 bedforms, such as step-pools, developed. Large clasts are not even transported by the Q_{50} flow,
675 although some rotation and imbrication occurred at the highest flows. Thus the large clasts create
676 fixed constrictions that the remainder of mobile sediment and potential instream wood and log
677 jams form around. Even channel morphologies of steep alluvial channels (plane bed, step-pool,
678 and cascades) are most likely controlled by the location of lateral constrictions and coarse
679 sediments (Vianello & D'Agostino, 2007), and flow convergence at channel constrictions in
680 pool-riffle channels play a major role in sediment routing and backwater development
681 (Thompson & Wohl, 2009). Therefore, it is not surprising that immobile boulders would play a
682 large role in the organization of the entire channel morphology. Thus neither Montgomery &
683 Buffington's (1997) or Palucis & Lamb's (2017) general patterns regarding correlations between
684 bedforms and slope apply in this environment. According to Montgomery & Buffington's (1997)
685 bedform scheme, step-pools form in supply-limited systems. However, the setting for the
686 prototype streams are severely transport-limited system due to the non-flashy hydrological
687 regime, where very high magnitude flows are limited due to mainstem lakes and the unconfined
688 valley geometries. Furthermore, channel widths may be too large to promote boulder jamming
689 and thus step formation (Zimmerman et al., 2010).

690   Although no channel-spanning bedforms developed, there were patterns of sediment
691 deposition and scour in relation to large clasts. These patterns are in accordance with previous
692 studies on boulder-bed channels with low relative submergence regimes, where sediment will
693 deposit upstream of large immobile boulders (Monsalve & Yager, 2017; Papanicolaou et al.,
694 2011, 2018). However, in this study, this pattern was only observed at the highest flows (Q_{10} and
695 Q_{50}) when large clasts were fully submerged but still with very low RS values (1-1.3). At lower
696 flows (Q_1 and Q_2) where large clasts protruded above the water surface elevation and fully
697 turbulent and hydraulically rough flows had not developed, more sediment deposited
698 downstream of large clasts. After the Q_{10} and Q_{50} flows at both slope setups, sediment clusters of
699 fine- to medium- sized sediment (D_{10} and D_{50}) formed upstream of large clasts. Previous flume
700 experiments have examined the role of individual boulders on sediment deposition and have
701 measured the hydraulics around large clasts in low RS (LRS), in terms of velocity, shear stress,
702 and shear stress divergence. Monsalve and Yager (2017) observed sediment deposition upstream
703 of large clasts and scour between clasts, which they explained formed as a result of negative bed
704 shear stress divergence within a medium range of shear stress magnitudes so that size-selective
705 entrainment is possible, in addition to the direction of bed shear stress vectors. Papanicolaou et
706 al. (2018) note that the reversal in depositional locations in high RS (HRS) versus LRS
707 environments can be due to differences in the turbulent vortex structures and that the area or

708 length of these structures relative to clasts may affect depositional areas. Furthermore, at LRS,
709 the Froude number determines the location of sediment deposition: at subcritical flows, sediment
710 deposits in the stoss of boulders but at supercritical flows, sediment can deposit at the upstream
711 flanks of boulders (Papanicolaou et al., 2018). This pattern of upstream flank depositional zones
712 was also observed in this study at the Q_{10} flow at the 5% slope, where local areas of supercritical
713 flow with small hydraulic jumps were observed.

714   These previous flume studies of the effects of boulders in LRS regimes provide valuable
715 insights into hydraulics and mechanisms of sediment deposition around boulders in LRS streams
716 (e.g., Monsalve & Yager, 2017; Papanicolaou et al. 2011, 2018); however, in order to isolate the
717 effects of individual boulders, these experiments represented oversimplified conditions than
718 those found in the field in terms of boulder spacing and sediment size distribution. This study
719 adds several layers of complexity that more accurately reflects field conditions of semi-alluvial
720 channels by using a scaled down sediment distribution from field conditions of a prototype
721 stream (Figure 4f), rather than a bimodal bed vs. boulder sediment distribution. Also, in contrast
722 to previous studies where simple bed configurations were used, with isolated flow regimes where
723 wakes do not interfere with those of consecutive boulders, boulders in this study were randomly
724 located throughout the channel. Therefore, the data showed a large range in mean
725 aggradation/degradation upstream and downstream of large clasts, as the stoss or lee side of one
726 clast may be experiencing the effects of a proximal boulder located upstream, downstream or
727 even laterally. Although a more controlled study can yield interesting data on hydraulic effects of
728 single boulders, this study provides results that reflect the complexity and variability in field
729 conditions. Therefore, even with large variation, statistically significant differences in the
730 amount erosion/deposition around boulders can provide general trends of sediment patterns
731 around boulders. Future work should expand on the detailed hydraulic measurements around
732 boulders where large clasts are unevenly spaced, affecting one another, and have a wider grain
733 size distribution, in order to determine the length and area of turbulent vortex structures around
734 clasts (per Papanicolaou et al., 2018) and how they interact with one another to determine the
735 areas of sediment deposition relative to large clasts.

736   The protrusion of large boulders can play an important role in determining potential
737 sediment transport (Yager et al., 2007, 2012). Yager et al. (2007) found that protrusion of
738 immobile grains determines the shear stress available to transport mobile sediment. Furthermore,
739 protrusion decreases when sediment is deposited which in turn increases velocities and shear
740 stress available to transport sediment. There is insufficient data in this experiment to determine
741 whether there was a feedback in degree of protrusion, aggradation, and potential for further
742 sediment transport. However, smoothing of the longitudinal profile, visualized through increased
743 elevations upstream and downstream of protrusions suggest a decrease in protrusion (Figure S4).

744 4.3 Widespread distribution of semi-alluvial channels

745   Previous work on semi-alluvial channels have focused nearly solely on those with a mix
746 of alluvial and bedrock elements, with either the channel bank or bed composed of bedrock
747 (Turowski, 2012). However, few studies have examined sediment organization in semi-alluvial
748 channels where immobile sediment reduce potential sediment transport and influence sediment
749 cluster formation. As most fluvial geomorphic studies have been conducted in temperate zones,
750 beyond the limit of continental glaciation, or in mountain environments that are usually supply-

751 limited, the sediment transport literature has focused on alluvial channels. The widespread
752 distribution of continental glaciation-related till at northern latitudes probably means that
753 boulder-bed semi-alluvial channels may also be widespread. Systematic global mapping of these
754 channel types is lacking; however, mapping of Canadian channel types suggest that semi-alluvial
755 streams are common in large parts of the Canadian Shield (Ashmore & Church, 2001).
756 Understanding these boulder-bed semi-alluvial channels bridges previous research on semi-
757 alluvial bedrock channels or low-gradient channels cut into peat or lacustrine sediment with that
758 of steep coarse-bed channels in young mountain ranges. Even in young mountain ranges,
759 hillslope-derived blocks (>1 m) can slow the rate of channel incision (Shobe et al., 2016), and
760 thus could also be described as semi-alluvial.

761   Furthermore, at northern latitudes, mainstem lakes are widespread (Messager et al.,
762 2016). With the exception of studies on the effects of lakes on sediment size in Maine, U.S.A.
763 (Snyder et al., 2012) and the effect of lakes on downstream hydraulic geometry in Idaho, U.S.A.
764 (Arp et al., 2007), the effect of lakes on geomorphic channel dynamics is little studied. Mainstem
765 lakes buffer downstream sediment transport and will decrease the fine sediment available to be
766 re-worked in a semi-alluvial rapid reach (Arp et al., 2007; Synder et al., 2012). In Fennoscandia,
767 this decrease in available fine sediment is exacerbated by the overall low sediment yield on the
768 continental shield due to the crystalline bedrock, cold climate and generally low relief (Polvi et
769 al. 2020). These conditions that lead to low sediment yields are also common in the boreal shield
770 regions of Canada, and may translate to similar low sediment yield stream systems. Fine
771 sediment can only be recruited from channel banks and local tributary junctions. This
772 interpretation is supported by analyses of sediment yields in Canada that show that sediment
773 yield increases disproportionately with drainage area because sediment is eroded directly from
774 streambanks. This indicates that rivers are degrading and that streams are eroding through
775 Quaternary deposits of glacial sediment (Church et al. 1999). In addition to streambank
776 sediment, some prototype reaches produce additional fine sediment from pre- or interglacially
777 highly weathered bedrock or boulders of Revsunds granite (*personal observation*; *personal
778 communication*, Rolf Zale). If greater amounts of fine sediment (sand to medium gravel) were
779 available, it is possible that different patterns of deposition in relation to boulders would result.

780 4.4 Implications for restoration

781   In the past two decades, semi-alluvial rapids have been targeted for restoration, with
782 >100 million Euro being spent to improve trout and salmon habitat in Sweden and Finland (e.g.,
783 Gardeström et al., 2013); however, positive ecological results have been sparse (Nilsson et al.,
784 2015). Restoration has included increasing geomorphic complexity by adding large boulders, in
785 addition to opening side channels and removing small dams, followed by adding spawning
786 gravel downstream of boulders. However, based on the results from this flume experiment, to
787 ensure the longevity of spawning beds, spawning gravel should not always be placed in
788 downstream wakes in channels with low relative submergence regimes. In contrast to alluvial
789 channels, the channel will likely not re-organize the restored major bed elements such as coarse
790 boulder. Therefore there is a larger burden on restoration practitioners to restore these streams
791 correctly, in terms of balancing erosion and deposition and creating appropriate microhabitat.

5 Conclusions

This flume experiment was designed to elucidate how semi-alluvial boulder-bed channels with a snowmelt-dominated flow regime evolve in terms of potential bedforms or sediment clusters. These channels have a coarse sediment distribution, resembling that of steep mountain streams, but previous field observations have suggested that these channels do not form bedforms found in gravel-bed alluvial channels (*sensu* Montgomery & Buffington, 1997). My results confirmed that even 50-year flow events do not reorganize bed sediment to form regular bedforms. However, patterns in sediment deposition were found in relation to boulders ($>D_{84}$): at moderate to high flows (Q_{10}-Q_{50}), finer sediment is deposited upstream of boulders rather than in downstream wakes. Because the geomorphic work done by the Q_{50} flow is less than that of the bankfull or annual high-flow event (Q_1), it shows that the Q_{50} flow would not be able to disrupt grain interlocking and thus re-organize bedforms or boulders. This finding places these boulder-bed semi-alluvial channels in a different category than mountain streams, where many step-pool channels re-organize steps every 10-50 years (e.g., Bunte et al., 2014; Turkowski et al., 2009). These results lead to the conclusion that the channel geometry of these semi-alluvial channels do not reflect equilibrium conditions based on the current snowmelt-dominated flow regime and sediment regime. The results from this study, combined with low-magnitude high-recurrence flows, due to mainstem lakes that buffer high flows and unconfined channel geometry, and the history of extremely high post-glacial flows, suggest that few channel-forming flows have occurred post-glaciation. Channels may instead have inherited their geometry from unsorted glacial sediment that was deposited from glacial meltwater sub-glacially or downstream of melting glaciers ca. 9000-10000 y. B.P.

Recently, the importance of large grains in controlling processes in gravel-bed streams has gained prominence in the scientific literature (e.g., Williams et al., 2019). For example, MacKenzie and Eaton (2017) found that a slight increase in the D_{90} of a sediment size distribution caused a four-fold decrease in sediment transport. Rather than relying on the classic median grain size to determine sediment transport processes and channel morphology, MacKenzie et al. (2018) encourage us to examine the mobility of the largest grains in order to understand channel morphology. Similarly, Yager et al. (2018) argue that grain resistance, in particular that of large boulders that protrude from the channel, serve to increase the dimensionless critical shear stress so that the sediment transport threshold varies substantially among streams. Given these insights into the role of large grains in shaping sediment transport processes and thus channel morphology, semi-alluvial channels with abundant boulders relative to their transport capacity may form quite unique morphologies compared to alluvial channels.

Acknowledgments

835 several volunteers who helped set up the flume and carry out the experiments: William
836 Amponsah, Truxton Blazek, Margherita Righini, Daniel Scott, Katherine Lininger, and Susan
837 Cundiff. Thank you to Gabrielle David who commented on an earlier draft of the manuscript.
838 Finally, I thank Peter Ashmore, Rob Ferguson and an anonymous reviewer whose constructive
839 comments have greatly improved the manuscript.

840 **References**

841 Agisoft LLC. (2014). St. Petersburg, Russia.
842

843 Andrews, E. D. (1980). Effective and bankfull discharges of streams in the Yampa River Basin,
844 Colorado, and Wyoming. *Journal of Hydrology, 46*, 311–330.
845

846 Arnold, N., & Sharp, M. (2002). Flow variability in the Scandinavian ice sheet: modelling the
847 coupling between ice sheet flow and hydrology. *Quaternary Science Reviews, 21*, 485-502.
848 https://doi.org/10.1016/S0277-3791(01)00059-2
849

850 Arp, C. D., Gooseff, M. N., Baker, M. A., & Wurtsbaugh, W. (2006). Surface-water
851 hydrodyanamics and regimes of a small mountain stream-lake ecosystem. *Journal of Hydrology,
852 329*, 500-513. https://doi.org/10.1016/j.jhydrol.2006.03.006
853

854 Arp, C. D., Schmidth, J. C., Baker, M. A., & Myers, A. K. (2007). Stream geomorphology in a
855 mountain lake district: hydraulic geometry, sediment sources and sinks, and downstream lake
856 effects. *Earth Surface Processes and Landforms, 32*, 525-543. https://doi.org/10.1002/esp.1421
857

858 Ashmore, P., & Church, M. (2001). The impact of climate change on rivers and river processes
859 in Canada. *Geological Survey of Canada, Bulletin* 555, 58 pp.
860

861 Bathurst, J. C. (2002). At-a-site variation and minimum flow resistance for mountain rivers.
862 *Journal of Hydrology, 269*, 11-26. https://doi.org/10.1016/S0022-1694(02)00191-9
863

864 Bergstrand, M., Asp, S-S., & Lindström, G. (2014). Nationwide hydrological statistics for
865 Sweden with high resolution using the hydrogical model S-HYPE. Hydrology Research, 45, 349-
866 356. https://doi.org/10.2166/nh.2013.010
867

868 Boulton, G. S., Hagdorn, M., Maillot, P. B., & Zatsepin, S. (2009). Drainage beneath ice sheets:
869 groundwater-channel coupling, and the origin of esker systems from former ice sheets.
870 *Quaternary Science Reviews, 28*, 621-638. https://doi.org/10.1016/j.quascirev.2008.05.009
871

872 Bray, D. I. (1979). Estimating average velocity in gravel-bed rivers. *Journal of the Hydraulics
873 Division- ASCE, 105*, 1103-1122.
874

875 Brummer, C. J., & Montgomery, D. R. (2003). Influence of coarse lag formation on the
876 mechanics of sediment pulse dispersion in a mountain stream, Squire Creek, North Cascades,
877 Washington, United States. *Water Resources Research, 42*(7), W07412.
878 https://doi.org/10.1029/2005WR004776
879

880 Bunte, K., Abt, S. R., Swingle, K. W., & Cenderelli, D.A. (2014). Effective discharge in Rocky
881 Mountain headwater streams. *Journal of Hydrology, 519*, 2136-2147.
882 http://dx.doi.org/10.1016/j.jhydrol.2014.09.080

884 Chin, A., & Wohl, E. (2005). Toward a theory for step pool in stream channels, *Progress in
885 Physical Geography: Earth and Environment, 29*, 275–296.
886 https://doi.org/10.1191/0309133305pp449ra

888 Church, M. (2006), Bed material transport and the morphology of alluvial river channels, *Annual
889 Review of Earth and Planetary Sciences, 34*, 325-354.
890 https://doi.org/10.1146/annurev.earth.33.092203.122721

892 Church, M., Ham, D., Hassan, M., & Slaymaker, O. (1999). Fluvial clastic sediment yield in
893 Canada: scaled analysis. *Canadian Journal of Earth Sciences, 36*, 1267-1280.

895 Church M., & Zimmerman, A. (2007). Form and stability of step-pool channels: Research
896 progress. *Water Resources Research*, 43, W03415. https://doi.org/10.1029/2006WR005037

898 Coulombe-Pontbriand, M., & LaPointe, M. (2004). Geomorphic controls, riffle substrate quality,
899 and spawning site selection in two semi-alluvial salmon rivers in the Gaspé Peninsula, Canada.
900 *River Research and Applications, 20*, 577-590. https://doi.org/10.1002/rra.768

902 Curran, J. C., & Wilcock, P. R. (2005), Characteristic dimensions of the step-pool configuration:
903 An experimental study, *Water Resoures. Research, 41*, W02030,
904 https://doi.org/10.1029/2004WR003568.

905 David, G. C. L., Wohl, E., Yochum, S. E. & Bledoe, B. P. (2011). Comparative analysis of bed
906 resistance partitioning in high-gradient streams. *Water Resources Research, 47*, W07507.
907 https://doi.org/10.1029/2010WR009540

908 Downs, P.W., Soar, P.J., & Taylor, A. (2016). The anatomy of effective discharge: the dynamics
909 of coarse sediment transport revealed using continuous bedload monitoring in a gravel-bed river
910 during a very wet year. Earth Surface Processes and Landforms, 41, 147-161.
911 https://doi.org/10.1002/esp.3785

912 Emmett, W. W., & Wolman, M. G. (2001). Effective discharge and gravel-bed rivers. *Earth
913 Surface Processes and Landforms, 26*, 1369-1380. https://doi.org/10.1002/esp.303

914 Ettema, R., & Kempema, E.W. (2013). Ice effects on sediment transport. In *River Ice Formation
915 ED: Spyros, B. Pp.297-338. Published by the Committee on River Ice Processes and the
916 Environment, Canadian Geophysical Union Hydrology Section, Edmonton, Alberta, Canada
917 http://cripe.civil.ualberta.ca/*

919 ESRI (2017). ArcGIS Desktop: v. 10.5.1. Redlands, CA: Environmental Systems Research
920 Institute.
921

Faustini , J. M., Kaufmann, P. R., Herlihy, A. T. (2009). Downstream variation in bankfull width of wadeable streams across the conterminous United States, *Geomorphology, 108*, 292-311.

Gardeström, J., Holmqvist, D., Polvi, L.E., & Nilsson, C. (2013). Demonstration restoration measures in tributaries of the Vindel River catchment. *Ecology and Society, 18*(3), 8. http://dx.doi.org/10.5751/ES-05609-180308

Gran, K.B., Finnegan, N., Johnson, A. L., Belmont, P., Wittkop, C., & Rittenour, T. 2013. Landscape evolution, valley excavation, and terrace development following abrupt postglacial base-level fall. *Geological Society of America Bulletin, 125*, 1851-1864. http://dx.doi.org/10.1130/B30772.1

Grant, G.E. 1997. Critical flow constrains flow hydraulics in mobile-bed streams: A new hypothesis. Water Resources Research, 33, 349-358. http://dx.doi.org/10.1029/96WR03134

Hassan, M. A., Brayshaw, D., Alila, Y., & Andrews, E. (2014). Effective discharge in small formerly glaciated mountain streams of British Columbia: limitations and implications. *Water Resources Research, 50*, 4440-4458. http://doi/10.1002/2013WR014529.

Hendrick, R. R., Ely, L. L, & Papanicolaou, A. N. (2010). The role of hydrologic processes and geomorphology on the morphology and evolution of sediment clusters in gravel-bed rivers. *Geomorphology, 114*, 483-496. http://doi/10.1016/j.geomorph.2009.07.018

Herman, F., Beaud, F., Champagnac, J-D., Lemieux, J-M., & Sternai, P. (2011). Glacial hydrology and erosion patterns: A mechanism for carving glacial valleys. *Earth and Planetary Science Letters, 310*(3), 498-508. http://doi/10.1016/j.epsl.2011.08.022

Hey, R. D. (1979). Flow resistance in gravel-bed rivers. Journal of the Hydraulics Division-*ASCE, 105*, 365-379.

Jansen, J. D., Codilean, A. T., Stroeven, A. P., Fabel, D., Hättestrand, C., Kleman, J., et al. (2014). Inner gorges cut by subglacial meltwater during Fennoscandian ice sheet decay. *Nature Communications 5*, 3815. https://doi/10.1038/ncomms4815

Johnson, J. P. L. 2016. Gravel threshold of motion: a state function of sediment transport disequilibrium? *Earth Surface Dynamics, 4*, 685-703. https://doi/10.5194/esurf-4-685-2016

Julien, P. Y. (2002). *River Mechanics*. Cambridge, UK: Cambridge University Press.

Laronne, J. B., Garcia, C., & Reid, I. (2001). Mobility of patch sediment in gravel bed streams: patch character and its implications for bedload. In M. Paul Mosley (Ed.), *Gravel-Bed Rivers V* (pp. 249-289), Wellington, New Zealand: New Zealand Hydrological Society Inc.

Leach, J. A., & Laudon, H. (2019). Headwater lakes and their influence on downstream discharge. *Limnology and Oceanography Letters, 4*, 105-112. https://doi.org/10.1002/lol2.10110

958
959 Lee, A. J., & Ferguson, R. I. 2002. Velocity and flow resistance in step-pool streams.
960 Geomorphology, 46, 59-71. https://doi.org/10.1016/S0169-555X(02)00054-5
961
962 Lenzi, M. A. (2001), Step-pool evolution in the Rio Cordon, northeastern Italy. *Earth Surface*
963 *Processes Landforms,* 26, 991–1008. https://doi.org/10.1002/esp.239
964
965 Lenzi, M. A., Mao, L., & Comiti, F. (2006a). Effective discharge for sediment transport in a
966 mountain river: computational approaches and geomorphic effectiveness. *Journal of Hydrology,*
967 *325*, 257-276. https://doi/10.1016/j.jhydrol.2005.10.031
968
969 Lenzi, M. A., Mao, L., & Comiti, F. (2006b). When does bedload transport begin in steep
970 boulder-bed streams? *Hydrological Processes, 20*, 3516-3533. https://doi/10.1002/hyp.6168

971 Leopold, L. B., & Maddock, T. (1953). The hydraulic geometry of stream channels and some
972 physiographic characteristics. Geological Survey Professional Paper 252.

973 Lind, L., Alfredsen, K., Kuglerová, L., & Nilsson, C. (2016). Hydrological and thermal controls
974 of ice formation in 25 boreal stream reaches. *Journal of Hydrology, 540*, 797–811.
975 https://doi/10.1016/j.jhydrol.2016.06.053

976 Lindström, G., Pers, C. P., Rosberg, R., Strömqvist, J., & Arheimer, B. (2010). Development and
977 test of the HYPE (Hydrological Predictions for the Environment) model – A water quality model
978 for different spatial scales. *Hydrology Research, 41*(3-4), 295-319.
979 https://doi.org/10.2166/nh.2010.007

980 Lotsari, E., Wang, Y.S., Kaartinen, H., Jaakola, A., Kukko, A., Vaaja, M., Hyyppa, H., Hyyppa,
981 J., & Alho, P. (2015). Gravel transport by ice in a subarctic river from accurate laser scanning.
982 *Geomorphology, 246*, 113-122. https://doi.org/10.1016/j.geomorph.2015.06.009

983 Lundqvist, J. (1986). Late Weichselian glaciation and deglaciation in Scandinavia. *Quaternary*
984 *Science Reviews, 5*, 269-292.

985 Lvovich, M. I., Karasik, G. Y., Bratseva, N. L., Medvedeva, G. P., & Maleshko, A. V. (1991).
986 Contemporary Intensity of the World Land Intracontinental Erosion. Moscos: USSR Academy of
987 Sciences.

988 MacKenzie, L.G., & Eaton, B.C. (2017). Large grains matter: contrasting bed stability and
989 morphodynamics during two nearly identical experiments. *Earth Surface Processes and*
990 *Landforms, 42*, 1287-1295. https://10.1002/esp.4122

991 MacKenzie, L. G., Eaton, B. C., & Church, M. (2018). Breaking from the average: why large
992 grains matter in gravel-bed streams. *Earth Surface Processes and Landforms, 43*, 3190-3196.
993 https://doi.org/10.1002/esp.4465

994 Masteller, C. C., Finnegan, N. J., Turowski, J. M., Yager, E. M., & Rickenmann, D. (2019).
995 History-dependent threshold for motion revealed by continuous bedload transport measurements

996   in a steep mountain stream. *Geophysical Research Letters, 46*, 2583-2591. https://doi.org/
997   10.1029/2018GL081325

998   Meshkova, L. V., Carling, P. A., & Buffin-Bélanger T. (2012). Nomenclature, Complexity,
999   Semi-alluvial Channels and Sediment-flux-driven Bedrock Erosion, In M. Church, P. M. Biron,
1000   A. Roy (Eds.), *Gravel-bed Rivers: Processes, Tools, Environments, First Edition* (pp. 424-431).
1001   Chichester, UK: John Wiley & Sons, Ltd.

1002   Messager M. L., Lehner B., Grill G., Nedeva I. and Schmitt O. (2016). Estimating the volume
1003   and age of water stored in global lakes using a geo-statistical approach. *Nature Communications,*
1004   *7*, 13603. https://doi/10.1038/ncomms13603

1005   Monsalve, A., & Yager, E. M. (2017). Bed surface adjustments to spatially variable flow in flow
1006   relative submergence regimes. *Water Resources Research, 53*, 9350-6367.
1007   https://doi.org/10.1002/2017WR020845

1008   Montgomery, D. R. (1999). Process domains and the river continuum. *Journal of the American*
1009   *Water Resources Association, 35*(2), 397-410. https://doi/10.1111/j.1752-1688.1999.tb03598.x

1010   Montgomery, D. R., & Buffington, J. M. (1997). Channel-reach morphology in mountain
1011   drainage basins. *Geological Society of America Bulletin, 109*(5), 596-611.
1012   https://doi/10.1130/0016-7606(1997)109<0596:CRMIMD>2.3.CO;2

1013   Morgan, J. A., Brogan, D. J., & Nelson, P. A. (2017). Application of structure-from-motion
1014   photogrammetry in laboratory flumes. *Geomorphology*, *276*, 125-143.
1015   https://doi.org/10.1016/j.geomorph.2016.10.021

1016   Nilsson, C., Lepori, F., Malmqvist, B., Törnlund, E., Hjerdt, N., Helfield, J.M., et al. (2005).
1017   Forecasting environmental responses to restoration of rivers used as log floatways: an
1018   interdisciplinary challenge. Ecosystems, 8, 779–800. https://doi.org/10.1007/s10021-005-0030-9

1019   Nilsson, C., Polvi, L. E., Gardeström, J., Hasselquist, E. M., Lind, L., & Sarneel, J. M. (2015).
1020   Riparian and in-stream restoration of boreal streams and rivers: success or failure?
1021   *Ecohydrology, 8*(5), 753-764. https://doi.org/10.1002/eco.1480

1022   Nitsche, M., Rickenmann, D., Kirchner, J. W., Turowski, J. M., & Badoux, A. (2012).
1023   Macroroughness and variations in reach-averaged flow resistance in steep mountain streams.
1024   *Water Resources Research, 48*, W12518. https://doi.org/10.1029/2012WR012091

1025   Palucis, M.C., & Lamb, M.P. (2017). What controls channel form in steep mountain streams?
1026   *Geophysical Research Letters*, 44, 7245-7255. https://doi.org/10.1002/2017GL074198

1027   Papanicolaou, A. N., Dermisis, D. C., & Elhakeem, M. (2011). Investigating the role of clasts on
1028   the movement of sand in gravel bed rivers. *Journal of Hydraulic Engineering, 137*(9), 871-884.
1029   https://doi.org/10.1061/(ASCE)HY.1943-7900.0000381

1030   Papanicolaou, A. N., & Kramer, C. (2005). The role of relative submergence on cluster
1031   microtopography and bedload predictions in mountain streams. In G. Parker & M. H. Garcia

(Eds.), *4th IAHR symposium on river coastal and estuarine morphodynamics RCEM 2005* (pp. 1083- 1086).Urbana, IL: Taylor and Francis.

Papanicolaou, A. N., Kramer, C. M., Tsakiris, A. G., Stoesser, T., Bomminayuni S., & Chen, Z. (2012). Effects of a fully submerged boulder within a boulder array on the mean and turbulent flow fields: implications to bedload transport. *Acta Geophysica, 60*(6), 1502-1546. https://doi/10.2478/s11600-012-0044-6

Papanicolaou, A.N., Tsakiris, A.G., Wyssmanm, M.A., & Kramer, C.M. (2018). Boulder array effects on bedload pulses and depositional patches. *Journal of Geophysical Research- Earth Surface,* 123, 2925–2953. https://doi/10.1029/2018JF004753

Phillips, C. B., & Jerolmack, D. J. (2016). Self-organization of river channels as a critical filter on climate signals. *Science 352*, 694-697. https://doi/10.1126/science.aad3348

Pike, L., Gaskin, S., & Ashmore, P. (2018). Flume tests on fluvial erosion mechanisms in till-bed channels. *Earth Surface Processes and Landforms, 43*, 259-270.

Polvi, L.E. (2020). Morphology of boulder-bed semi-alluvial channel beds: a flume study modelling streams in northern Fennoscandia. Swedish National Data Service. https://doi.org/10.5878/kz4r-6y69 (Polvi, 2020).

Polvi, L.E., Dietze, M., Lotsari, E., Turowski, J.M., & Lind, L. (2020). Seismic Monitoring of a Subarctic River: Seasonal Variations in Hydraulics, Sediment Transport, and Ice Dynamics. *Journal of Geophysical Research- Earth Surface*, 125, e2019JF005333. https://doi.org/10.1029/2019JF005333

Polvi, L. E., Nilsson, C., & Hasselquist, E. M. (2014). Potential and actual geomorphic complexity of restored headwater streams in northern Sweden. *Geomorphology, 210*, 98-118. https://doi/10.1016/j.geomorph.2013.12.025

Reid, I., Frostick, F.E., Layman, J.T. (1985). The incidence and nature of bedload transport during flood flows in coarse grained alluvial channels. *Earth Surface Processes and Landforms, 10*, 33–44

Reid, H. E., Brierley, G. J., Mcfarlane, K., Coleman, S. E., & Trowsdale, S. (2013). The role of landscape setting in minimizing hydrogeomorphic impacts of flow regulation. International Journal of Sediment Research 28, 149-161. https://doi.org/10.1016/S1001-6279(13)60027-X

Rosenfeld, J., Hogan, D., Palm, D., Lundquist, H., Nilsson, C., & Beechie, T. J. (2011). Contrasting Landscape Influences on Sediment Supply and Stream Restoration Priorities in Northern Fennoscandia (Sweden and Finland) and Coastal British Columbia. Environmental Management, 47(1), 28-39. https://doi.org/10.1007/s00267-010-9585-0

RStudio Team (2016). RStudio: Integrated Development for R, v. 1.1.383. Boston, MA: RStudio , Inc. http://www.rstudio.com/

1067   Sear, D. (1996). Sediment transport processes in pool-riffle sequences. *Earth Surface Processes*
1068   *and Landforms*, 21, 241-262. https://doi/ 10.1002/(SICI)1096-9837(199603)21:3<241::AID-
1069   SP623>3.0.CO;2-1

1070   Seppälä, M. (2005). Glacially sculptured landforms, In M. Seppälä (Ed.), *The Physical*
1071   *Geography of Fennoscandia* (pp 35- 57). New York: Oxford University Press.

1072   Shobe, C.M., Tucker, G.E., & Anderson, R.S. (2016). Hillslope-derived blocks retard river
1073   incision. *Geophysical Res. Letters, 43*, 5070-5078. https://doi.org/ 10.1002/2016GL069262

1074   SMHI (2015). Vattenwebb: S-HYPE model data. Retrieved from http://vattenwebb.smhi.se/

1075   SMHI (2017). Swedish Meteorological and Hydrological Institute. Retrieved from
1076   http://www.smhi.se

1077   Stroeven, A. P., Hättestrand, C., Kleman, J., Heyman, J., Fabel, D., Fredin, O., et al. (2016).
1078   Deglaciation of Fennoscandia. *Quaternary Science Reviews, 147*, 91-121.
1079   https://doi.org/10.1016/j.quascirev.2015.09.016

1080   Snyder, N. P., Castele, M. R., & Wright, J. R. (2008). Bedload entrainment in low-gradient
1081   paraglacial coastal rivers of Maine, U.S.A.: implications for habitat restoration. *Geomorphology*
1082   *103*, 430-446. https://doi/10.1016/j.geomorph.2008.07.013

1083   Synder, N., Nesheim, A. O., Wilkins, B. C, & Edmonds, D. A. (2012). Predicting grain size in
1084   gravel-bedded rivers using digital elevation models: application to three Maine watersheds.
1085   Geological Society of America Bulletin. https://doi/10.1130/B30694.1

1086   Thompson, D. (2008). The influence of lee sediment behind large bed elements on bedload
1087   transport rates in supply-limited channels. *Geomorphology, 99*, 420-432.
1088   https://doi/https://doi.org/10.1016/j.geomorph.2007.12.004

1089   Thompson, D. M., & Wohl, E. E. (2009).The linkage between velocity patterns and sediment
1090   entrainment in a forced-pool and riffle unit. *Earth Surface Processes and Landforms, 34*, 177-
1091   192. https://doi/10.1002/esp.1698

1092   Torizzo, M., & Pitlick, J. (2004). Magnitude-frequency of bed load transport in mountain
1093   streams in Colorado. *Journal of Hydrology, 290*, 137-151.
1094   https://doi/10.1016/j.hydrol.2003.12.001

1095   Turowski, J. M. (2012). Semi-alluvial channels and sediment-flux-driven bedrock erosion. In M.
1096   Church, P. M. Biron, A. Roy (Eds.), *Gravel-bed Rivers: Processes, Tools, Environments, First*
1097   *Edition* (pp. 401-416). Chichester, UK: John Wiley & Sons, Ltd.

1098   Turowski, J. M., Yager, E. M., Badoux, A., Rickenmann, D., & Molnar, P. (2009). The impact of
1099   exceptional events on erosion, bedload transport and channel stability in a step-pool channel.
1100   *Earth Surface Processes and Landforms, 34*, 1661-1673. https://doi/10.1002/esp.1855

1101   Vianello, A., & D'Agostino, V. (2007). Bankfull width and morphological units in an alpine
1102   stream of the dolomites (northern Italy). *Geomorphology, 83*, 266-281.
1103   https://doi.org/10.1016/j.geomorph.2006.02.023

1104   Walling, D. E., & Webb, B. W., (1983). Patterns of sediment yield. In K. J. Gregory (Ed.),
1105   *Background to Palaeohydrology* (pp. 69-100). Chichester, UK: Wiley.

1106   Westoby, M. J., Brasington J., Glasser, N. F., Hambrey, M. J., & Reynolds, J. M. (2012).
1107   'Structure-from-Motion' photogrammetry: a low-cost, effective tool for geoscience applications.
1108   Geomorphology, 179, 300-314. https://doi.org/10.1016/j.geomorph.2012.08.021

1109   Wheaton, J. M., Brasington, J., Darby, S. E., & Sear, D. A. (2010). Accounting for uncertainty in
1110   DEMs from repeat topographic surveys: improved sediment budgets. *Earth Surface Processes*
1111   *and Landforms, 35*, 136-156. https://doi/10.1002/esp.1886

1112   Whittaker, J. G., & Jaeggi, M. N. R. (1982). Origin of step-pool systems in mountain streams,
1113   *Journal of the Hydraulic Division, ASCE, 108*, 758–773.

1114   Williams, R. D., Reid, H. E., & Brierley, G. J. (2019). Stuck at the bar: larger-than-average grain
1115   lag deposits and the spectrum of particle mobility. *Journal of Geophysical Research- Earth*
1116   *Surface, 124,* 2751-2756. https://doi.org/10.1029/2019JF005137

1117   Wolman, M. G., & Miller, J. P. (1960). Magnitude and frequency of forces in geomorphic
1118   processes. *J. Geol., 68*, 54–74.

1119   Yager, E. M., Kirchner, J. W., & Dietrich, W. E. (2007). Calculating bed load transport in steep
1120   boulder bed channels. *Water Resources Research, 43*, W07418.
1121   https://doi.org/10.1029/2006WR005432

1122   Yager, E. M., Turowski, J. M., Rickenmann D., & McArdell, B. W. (2012). Sediment supply,
1123   grain protrusion, and bedload transport in mountain streams. *Geophysical Research Letters, 39*,
1124   L10402. https://doi.org/10.1029/2012GL051654

1125   Yager, E. M., Schmeeckle, M. W., & Badoux, A. (2018). Resistance is not futile: grain resistance
1126   controls on observed critical shields stress variations. *Journal of Geophysical Research- Earth*
1127   *Surface, 123*, 3308-3322. https://doi.org/10.1029/2018JF004817

1128   Zimmermann, A., & Church, M. (2001). Channel morphology, gradient profiles and bed stresses
1129   during flood in a step-pool channel. *Geomorphology, 40*, 311–327.
1130   https://doi.org/10.1016/S0169-555X(01)00057-5

1131   Zimmermann, A., Church, M., & Hassan, M. A. (2010). Step-pool stability: testing the jammed
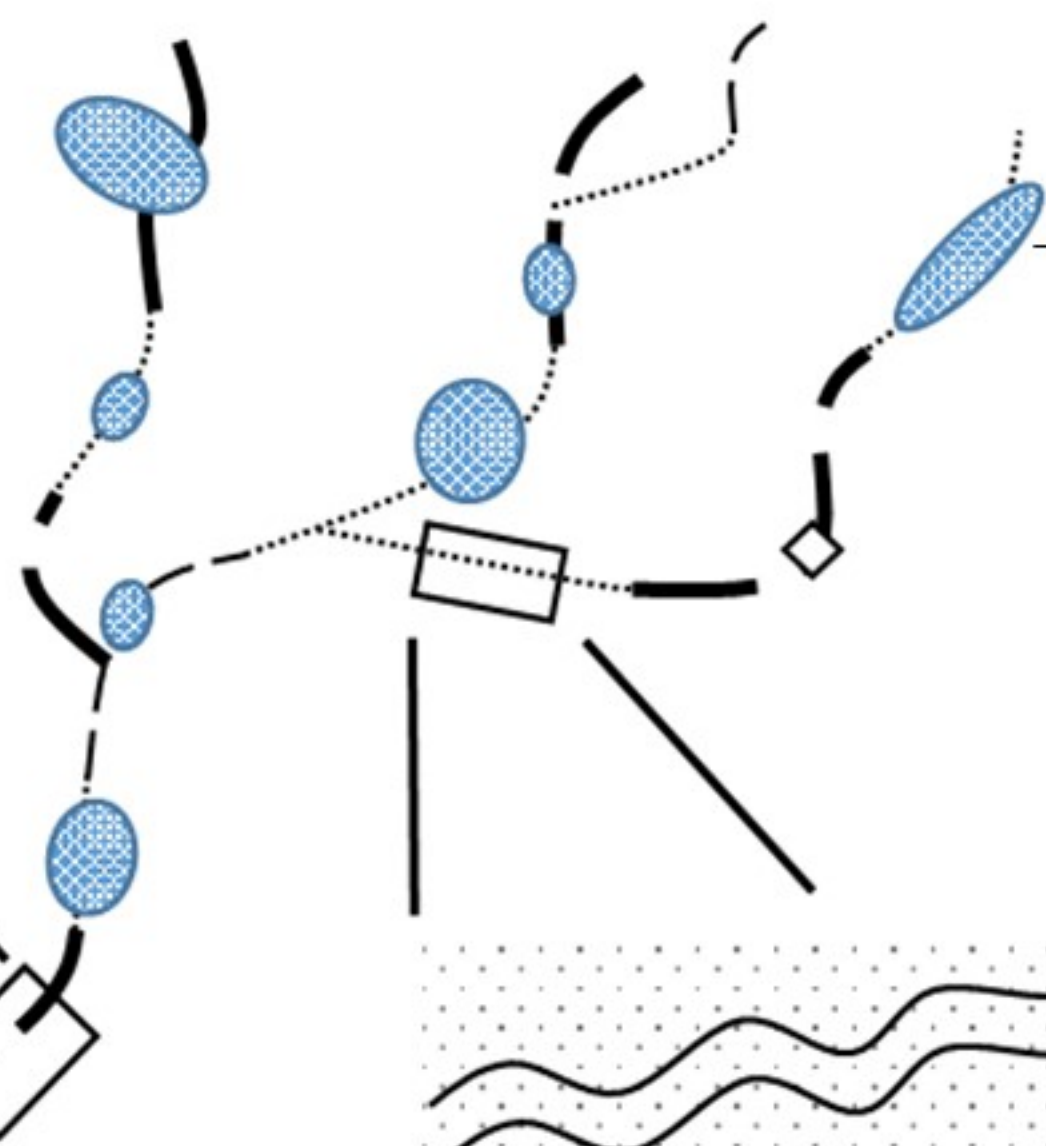1132   state hypothesis. *Journal of Geophysical Research- Earth Surface, 115*, F02008.
1133   https://doi.org/10.1029/2009JF001365

1134

1135

Figure 1.

a

~1 km

Lakes

Semi-alluvial rapids:
turbulent flow (S_0: 0.5-7%); with coarse boulders
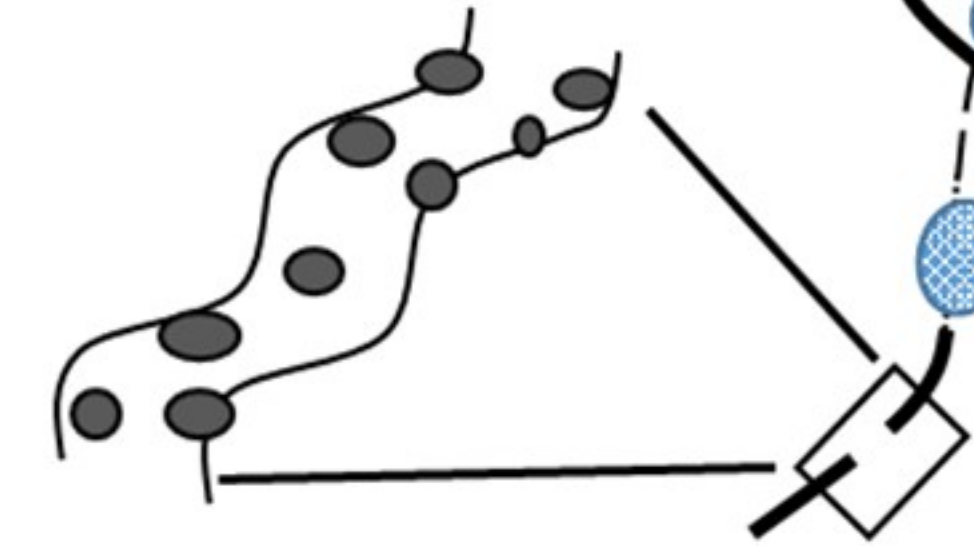
Slow-flowing reaches:
meandering/ straight channel (S_0 <1 %) in peat/ fine sediment

~10 m

~10 m

b

c

d

e

Figure 2.

Figure 3.
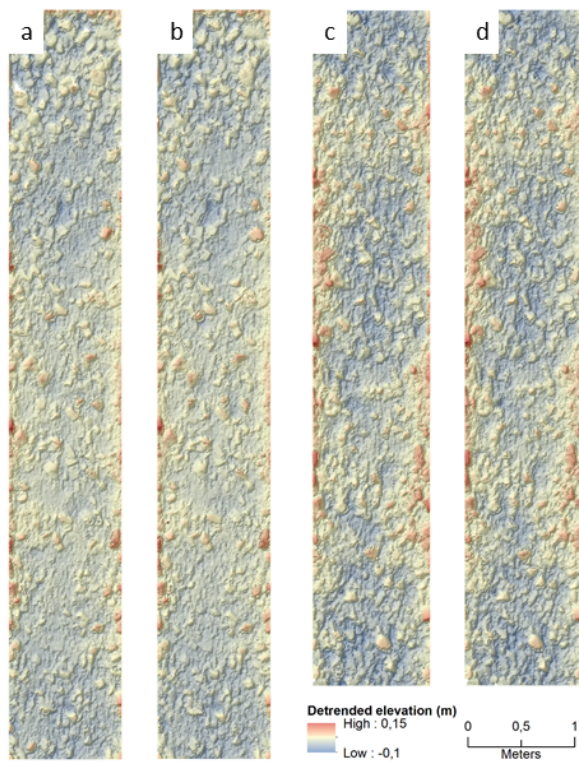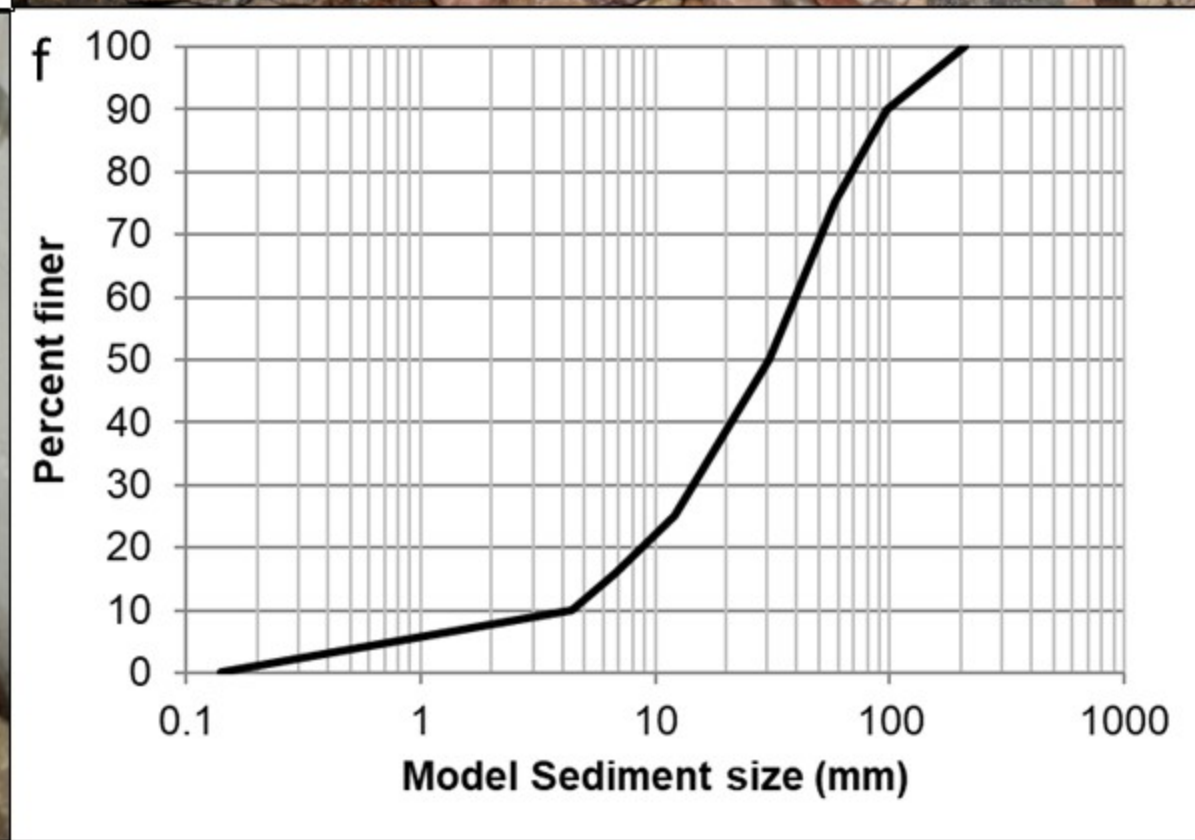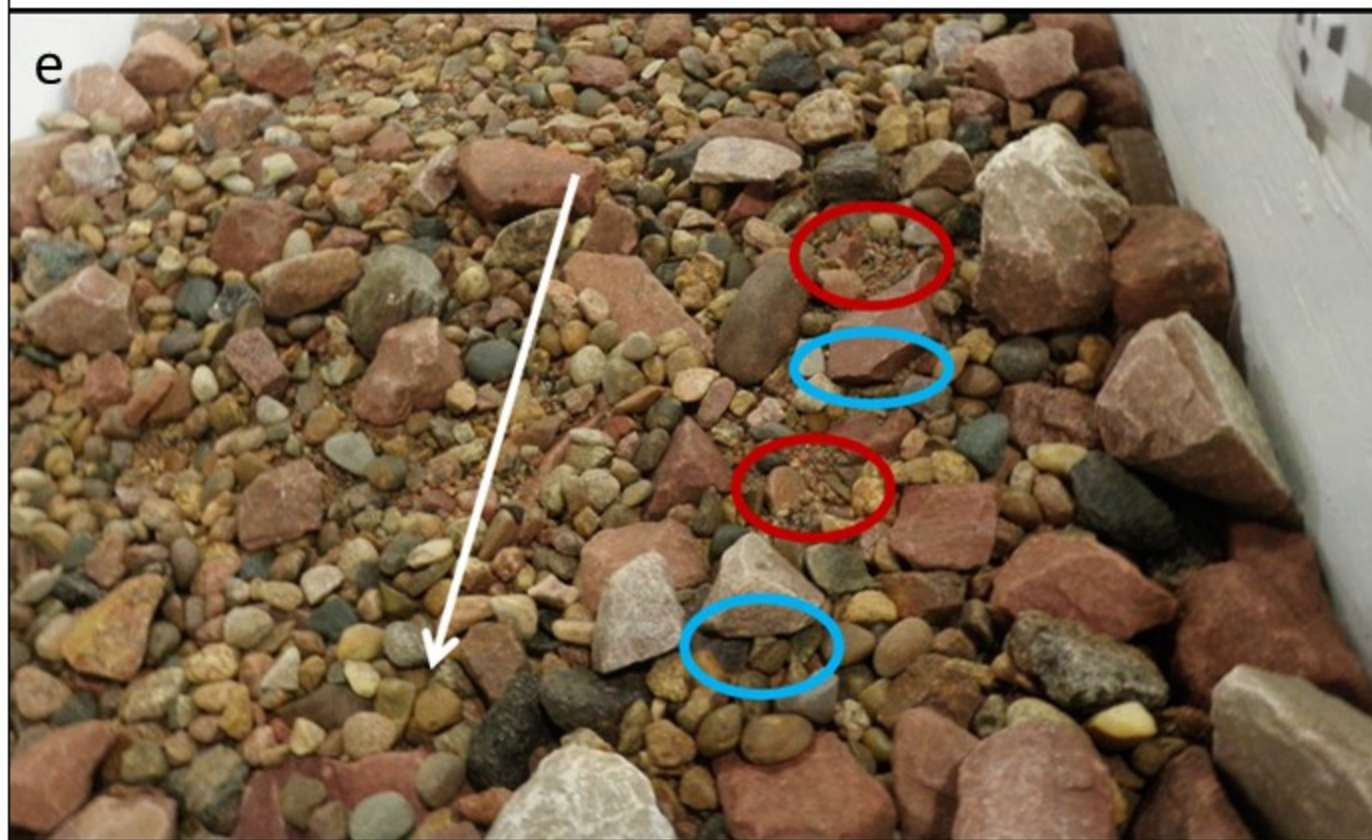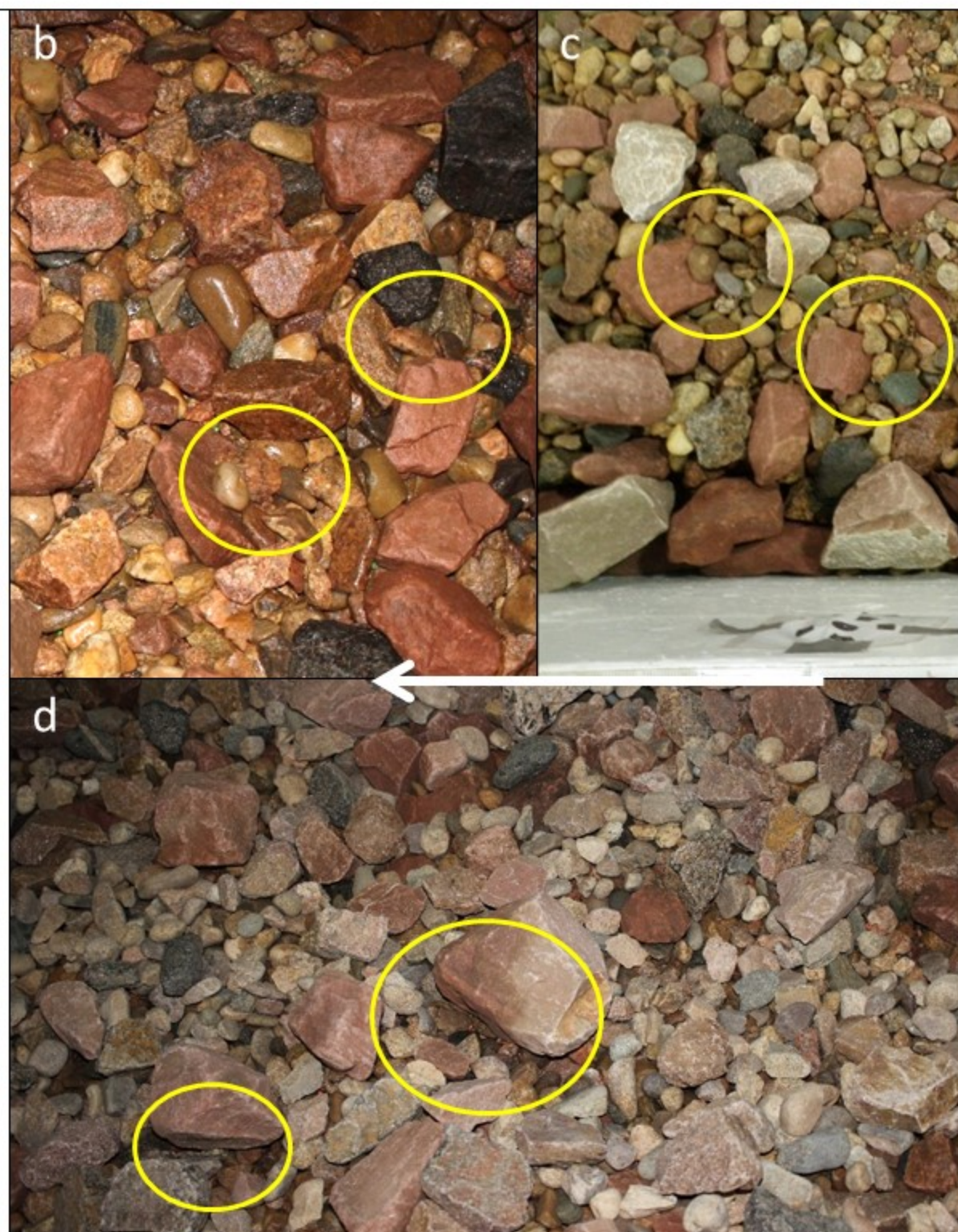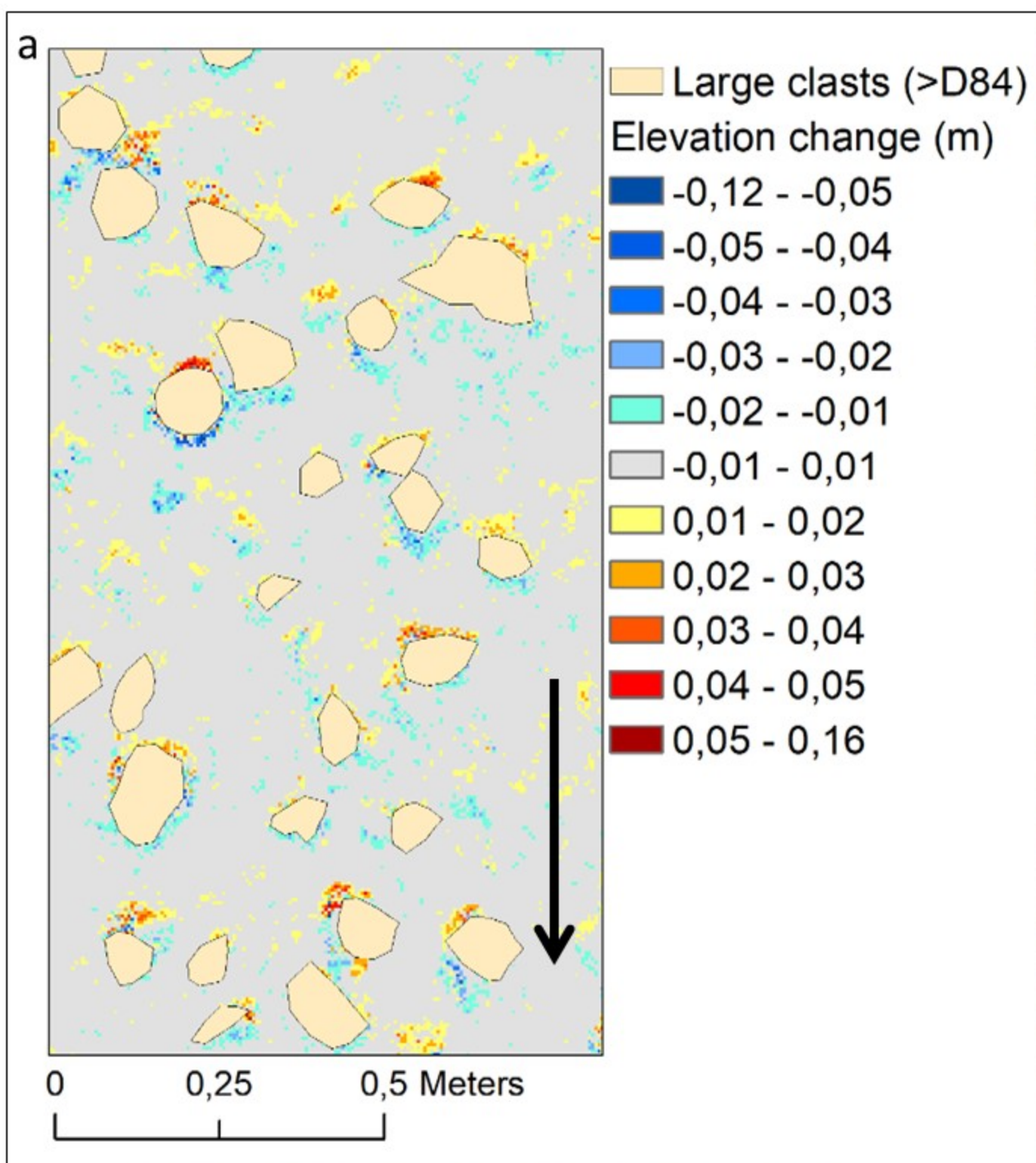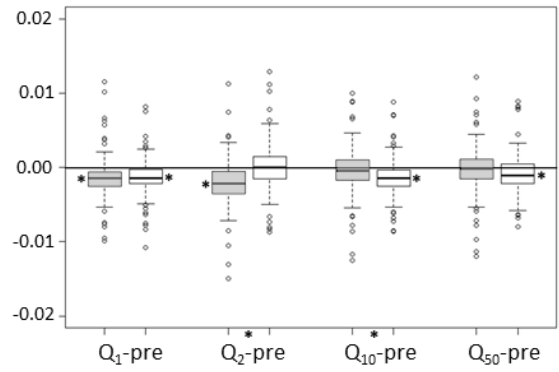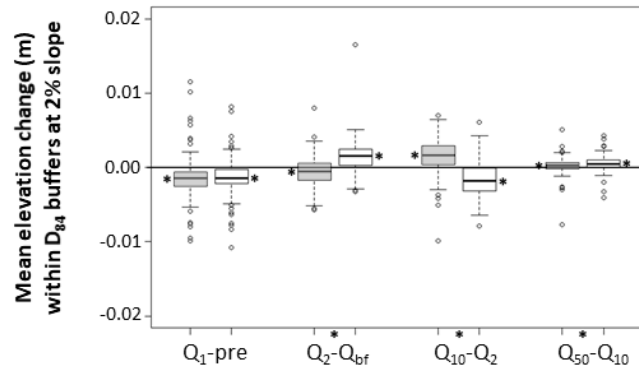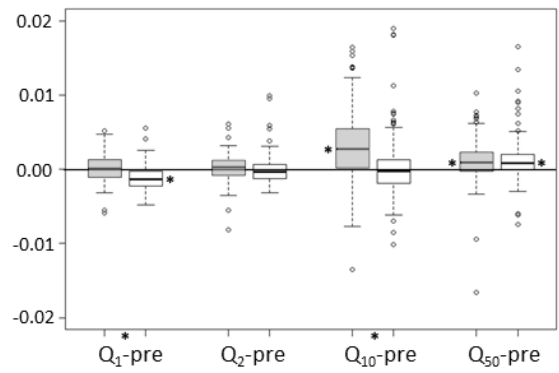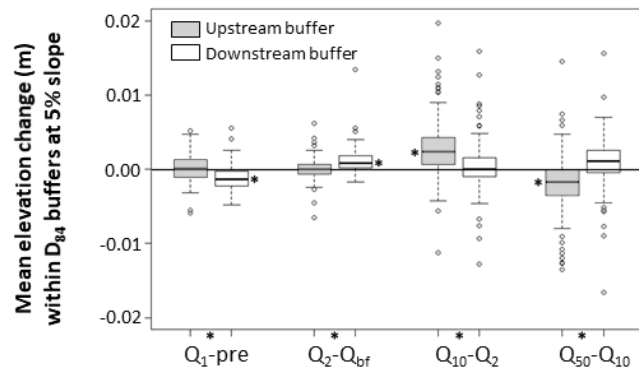
Detrended elevation (m)
High : 0,15
Low : -0,1

0   0,5   1
Meters

Figure 4.

Figure 5.

Table 3.

Slope	Pre-flow	Flow	Q (m³/s)	Std. Dev. DEM (m)	Flume area with deposition (%)[a]	Flume area with erosion (%)[a]	Flume area with erosion or deposition (%)[a]
2%		Pre		0.0228			
	Pre	Q_1	0.006	0.0231	4.83	9.80	14.63
	Q_1	Q_2	0.017	0.0228	1.58	5.55	7.13
	Q_2	Q_{10}	0.025	0.0229	7.60	7.91	15.51
	Q_{10}	Q_{50}	0.031	0.0228	4.32	3.40	7.73
5%		Pre		0.0304			
	Pre	Q_1	0.006	0.0308	5.85	7.07	12.92
	Q_1	Q_2	0.017	0.0307	6.08	4.93	11.01
	Q_2	Q_{10}	0.025	0.0306	11.26	7.48	18.74
	Q_{10}	Q_{50}	0.031	0.0303	9.52	10.39	19.92

[a] % area of deposition and erosion defined as area that experienced > 0.01 m net positive or negat

[b] Geomorphic work is defined as the cumulative sum of absolute values of aggradation and degrad

[c] Cumulative geomorphic work is defined as the sum for the given flow with all previous flows.

Volume of aggradation (m³)	Volume of degradation (m³)	Geomorphic work (m³)[b]	Cumulative geomorphic work (m³)[c]
0.013	-0.029	0.042	0.042
0.019	-0.017	0.036	0.079
0.022	-0.021	0.044	0.122
0.015	-0.013	0.028	0.150
0.017	-0.020	0.037	0.037
0.019	-0.015	0.034	0.071
0.006	-0.003	0.010	0.080
0.024	-0.027	0.050	0.131

ive elevation change.

ation after each flow.

Table 2.

Slope	Flow	Q (m³/s)	Stream power Ω (N/s)	Froude #	Mean flow depths (m)	Relative submergence (d/D84)	τ (N/m²)	Mobile sediment threshold (m) (τ*$_c$ = 0.045)
2%	Q$_{bf}$	0.006	1.18	0.47	0.024	0.31	4.48	0.006
	Q$_2$	0.017	3.34	0.45	0.049	0.63	8.87	0.013
	Q$_{10}$	0.025	4.91	0.41	0.068	0.87	11.83	0.018
	Q$_{50}$	0.031	6.08	0.42	0.078	1.00	13.36	0.021
5%	Q$_{bf}$	0.006	2.94	0.43	0.025	0.32	11.88	0.017
	Q$_2$	0.017	8.34	0.45	0.050	0.64	22.30	0.033
	Q$_{10}$	0.025	12.26	0.51	0.058	0.75	25.91	0.039
	Q$_{50}$	0.031	15.21	0.52	0.067	0.856	29.20	0.045

Mobile sediment threshold (m) ($\tau^*_c = 0.1$)
0.003
0.006
0.008
0.009
0.008
0.015
0.018
0.020